

Many-body theory of paired electron crystals

K. Mouloupoulos and N. W. Ashcroft

Laboratory of Atomic and Solid State Physics, Cornell University, Ithaca, New York 14853

(Received 21 May 1993)

We develop a variational many-body description of low-density three-dimensional paired electron crystals. Among the ground states of such crystals we find that coherent paired supersolids (resonant spin states) and true paired crystals (fixed spin states) can both be favored at intermediate densities ($100 \lesssim r_s \lesssim 200$) relative to the well-known conventional (Bravais lattice) Wigner crystals. The stabilization of this pairing is largely exchange driven and if it persists at higher densities (even beyond melting) then we show that for an intermediate density electron fluid an evolution into a superconducting state of unusual character can occur.

I. INTRODUCTION

As a problem in classical physics, it is well known that a static macroscopic assembly of N point charges ($-e$), placed in a homogeneous rigid background occupying volume V and possessing a total charge $+Ne$, acquires a minimum energy when the point charges are placed on the sites of a crystal, the crystal of lowest energy being the body-centered cubic (bcc), a Bravais lattice in its own right. Perhaps less well known is the fact that exceedingly close in energy can be found crystals that depart from the requirement that a single charge be placed in a unit cell. An important symmetric example for the quantum problem that we discuss below is the Pa3 structure (sometimes called the $\alpha-N_2$ structure): it is most easily viewed by imagining the steps followed in constructing a face-centered-cubic (fcc) crystal. Here spherically symmetric objects (the charge distributions around each site) are situated at the corners and face centers of a cube of side a [see Fig. 1(a)]. The fcc can be viewed therefore as a simple cubic with a four point basis, $(a/2)(1,1,0)$, $(a/2)(0,1,1)$, $(a/2)(1,0,1)$, and $(a/2)(0,0,0)$. To obtain the Pa3 structure, however, it is only necessary to remove the restriction to spherically symmetric objects; in fact, they are merely replaced by objects composed themselves of basis pairs, each consisting of two sites with separation $2d$, but with each of the four pairs oriented along

the four possible choices of body diagonal for the original cube [see Fig. 1(b)]. If the unit charges $-e$ are now situated at these basis points, and the electrostatic energy determined as a function of $2d$, then for fixed a the minimizing energy occurs at $d \approx 0.27a$; remarkably, it is only 3 parts in 1000 higher than the monatomic or Bravais lattice case. More interestingly still, at the minimizing value of d the pair separation $2d$ is actually *smaller* than the near-neighbor separation in a bcc structure with the same overall density [see Fig. 1(c)]. And even though the Madelung energy has risen by such a slight value (over the bcc minimum) the lowest *interpair* spacing [BC in Fig. 1(b)] is even shorter still, an observation of crucial importance when exchange is considered.

The energy we are discussing is the Madelung energy. If we define r_s by $(4\pi/3)r_s^3 a_0^3 = V/N$, then quite generally the Madelung energy per particle can be written as $(-\alpha/r_s)e^2/2a_0$, where α is the structure-dependent Madelung constant. The observation made above can be summarized by saying that for bcc, $\alpha_{\text{bcc}} = 1.79186$, whereas for a *paired* (Pa3) structure the value is $\alpha_{\text{Pa3}} = 1.78627$ for the minimizing choice of $2d = 0.54a$. The term pairing is apt here because, as is well known, the Pa3 structure can itself be obtained from a Bravais lattice, in this case a simple cubic (of side $a/2$) corresponding to $d = \sqrt{3}/4a$, and a less favorable Madelung constant $\alpha_{\text{sc}} = 1.76012$, by continuous decrease of the dis-

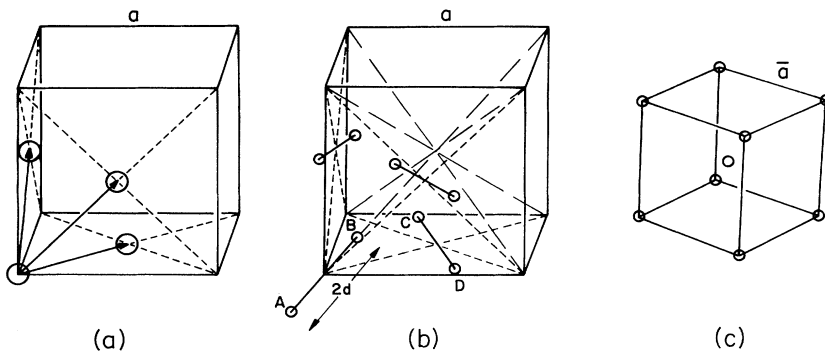


FIG. 1. (a) Face-centered cubic (fcc); (b) Pa3 ($\alpha-N_2$) structure with an intrapair distance $2d$; (c) body-centered cubic (bcc) for the same overall density as the structure in (b).

tance $2d$ [from $(\sqrt{3}/2)a \simeq 0.866a$ to the value $0.54a$ where the energy is lowest] along the cube diagonals. In a band context this would be a very straightforward way of rendering a three-dimensional Peierls transition.

Far from the ground state, in fact in the *classical* statistical mechanics of point charges in a rigid compensating background, the bcc structure again appears in the crystalline phase that commonly occurs upon freezing. The question we pose here concerns, however, the nature of crystalline phases in the ground state of a fully quantum-mechanical problem of fermionic point charges (electrons of mass m , for example). Specifically, we ask whether in a range of densities the role of *exchange* and *correlation* can overcome the relatively minor electrostatic penalty associated with Pa3 or similar structures (other competitive paired structures include Ga-type structure, the A-7 structure, etc.) in order to form a paired crystal. In principle the ground-state energy of the fully quantum-mechanical problem for electrons of mass m can be obtained through an integration over the mass starting from the pure electrostatic limit (corresponding to infinitely massive electrons), namely

$$\langle H \rangle_m = \langle H \rangle_\infty - \int_\infty^m dm' \frac{\langle T \rangle_{m'}}{m'},$$

with $\langle T \rangle_{m'}$ the kinetic energy for any intermediate mass m' . This is basically a form of the well-known Pauli theorem, but here involving an integration over one-body terms only. The above avoids calculation of the complicated two-body terms associated with the potential energy, and for the case of a harmonic monatomic crystal in the spherical cell approximation, where the width of the Gaussian orbitals can be easily determined in closed form as a function of the mass and the density, it gives immediately the correct ground-state energy. But for a paired case it is not immediately useful, since the kinetic energy is now a more complicated function of widths and of the pair size, and the dependence of these parameters on the mass is not at once known. However, we shall see that it is possible to determine $\langle H \rangle_m$ directly at the actual value of the mass m , since it is possible to evaluate in closed form both one-body and two-body terms as functions of the various parameters, and at the end make a variational determination of the actual values of those parameters. Following such a procedure, we shall see that provided the density is neither too low nor too high, paired structures are highly likely in three dimensions. The possibility of a paired crystal was discussed recently¹ in an effective single-cell approach for orientationally averaged paired structures. In that work the crucial many-body description developed here in detail (see Sec. III below) was also given [Eq. (20)]. The possibility of electron pairs occurring in a crystalline environment was first raised by Shuster and Kozinskaya,² though not quite in the context that we mean (for example, they only considered states with fully rotational character, with no classical limit). Their work suggested pairs at very high densities, which in retrospect is unrealistic. Also a paper recently appeared³ that adopts a description of spin-singlet localized pairs in terms of single-particle states, in basically the same way as the one we follow in Sec.

III B 2. However, the conclusions of Ref. 3 are rather different from ours, because of the extreme simplifying approximations made in the final discussion section of that paper. We return to this point in Sec. IV.

The Hamiltonian for our system is well known, simple, and highly symmetric. If \mathbf{r}_i are electron coordinates and $\rho = N/V$ the mean density, then

$$H = \sum_{i=1}^N \frac{p_i^2}{2m} + \frac{1}{2} \int d^3r \int d^3r' [\hat{\rho}^{(2)}(\mathbf{r}, \mathbf{r}') + \rho^2 - 2\rho \hat{\rho}^{(1)}(\mathbf{r})] v_c(\mathbf{r} - \mathbf{r}') \quad (1)$$

with $v_c(\mathbf{r}) = e^2/|\mathbf{r}|$, and where the two- and one-particle density operators are defined respectively by

$$\hat{\rho}^{(2)}(\mathbf{r}, \mathbf{r}') = \hat{\rho}^{(1)}(\mathbf{r}) \hat{\rho}^{(1)}(\mathbf{r}') - \delta(\mathbf{r} - \mathbf{r}') \hat{\rho}^{(1)}(\mathbf{r}') \quad (2)$$

and

$$\hat{\rho}^{(1)}(\mathbf{r}) = \sum_{i=1}^N \delta(\mathbf{r} - \mathbf{r}_i). \quad (3)$$

There is no explicit dependence on spin. For homogeneous phases [$\langle \hat{\rho}^{(1)}(\mathbf{r}) \rangle = \rho$ and $\langle \hat{\rho}^{(2)}(\mathbf{r}, \mathbf{r}') \rangle = \rho^{(2)}(|\mathbf{r} - \mathbf{r}'|) = (\rho)^2 g(\mathbf{r} - \mathbf{r}')$] the ground-state energy of (1) is

$$\langle H \rangle = \langle T \rangle + \frac{N}{2} \int d^3r \rho v_c(r) [g(r; r_s) - 1] \quad (4)$$

and the evaluation of (4) by a variety of techniques constitutes the interacting electron gas problem. But it was Wigner⁴ who first pointed out that solutions to (1) are possible that have an entirely different character; the symmetry of (1) is broken to form what has become known as the Wigner crystal. Wigner likened the states, localized quantal electrons in a uniform positive background, to an "inverse alkali metal," and proposed therefore a bcc structure. (Nowadays we know⁵ that the light alkali metals break the bcc structure even further in proceeding to their ground states.) A single unit cell in Wigner's crystal would be charge neutral, and accordingly will present outside it only weak multipole forces to other cells. The dynamics of a localized electron inside will therefore be almost entirely determined by the potential of a single reasonably spherical object with a uniform distribution of charge. This is harmonic and leads to a Gaussian distribution of charge for the electron itself. Providing this does not "leak" outside the cell (a simple condition on ρ) the entire argument can be made self-consistent: at low enough densities the system is therefore expected to crystallize. Spin, which does not enter (1) directly, is accommodated in the crystalline state by proposing a simple antiferromagnetic arrangement. As we shall see, its proper treatment is an extremely interesting problem.

It cannot be emphasized too strongly that the long-range nature of the interactions in the problem plays an essential role; this is clear from the proximity of the Madelung energies in the Bravais and non-Bravais lattice examples above. The problem therefore bears little similarity to the possibility of pairing in fermion systems where the effective interactions are *a priori* short ranged. The classic example is He^3 , though even here it may be

noted that while at low densities, He³ takes up a bcc structure, at higher densities it also transforms⁶ to a structure with two atoms per unit cell (hexagonal close packed) and hence possesses an internal parameter. In this system, exchange effects are said to be a relatively minor issue in the energetics of the structured phases. This is indeed the case, but the origin of this is very much tied to the short-ranged nature of the interaction, as will become evident below (the problem is treated briefly in Appendix C). For the charged paired system we reemphasize that exchange (or, better, the imposition of the antisymmetry on the many-body wave function) plays a quite central role, as we shall see. In fact, the spin character of such a phase can lead to energy gain in a way that generalizes the familiar concept of a superconducting diffusive electron system to a paired localized system with properties more reminiscent (and actually more general than that) of a supersolid,⁷ where coherent neutral lattice bosons (as in He⁴) are now replaced by charged paired fermions, whose internal structure is of vital importance. In this phase we have the interesting coexistence of two types of order, namely off-diagonal long-range order (associated with the pairing coherence) and diagonal long-range order (associated with the underlying lattice structure).

There are various ways of approaching the question of possible paired phases for electron crystals. Among the conventional treatments are collective methods (i.e., phonon sums for the energy of the actual lattice with the paired basis) which, however, violate the principle of indistinguishability and within which it is difficult to incorporate exchange, a special focus here as we have already noted. We therefore settle on an Einstein oscillator approach that, so far as exchange (both intra- and intercell) is concerned, constitutes the most rigorous approach and specifically focuses on the spin characteristics of the state. The intercell *dynamical* correlations (i.e., the consideration of the detailed *phonon* dispersions of the actual paired crystal) neglected in such a picture are expected to give contributions of only 3 parts in 10 000 (as, for example, in the calculation⁸ of the energy in the bcc structure, where the correction for phonon dispersion is $\sim 0.3/r_s^{3/2}$ with $r_s > 100$). This is an entire order of magnitude lower than the effects we discuss here. The reason for this is a combination of the Kohn sum rule⁹ according to which the sum of the squares of the phonon frequencies for a Coulomb lattice is a constant equal to the square of the plasma frequency, and the Domb-Salter relation¹⁰ according to which, for symmetric structures, the phonon energy is proportional to the square root of the second moment of the phonon spectrum, with the proportionality constant being quite insensitive to the structure.

In following this Einstein picture approach we use the second quantized version of (1) and therefore treat exchange between electrons completely; we find that this exchange may offer a mechanism for pairing at least in the localized case. Auxiliary material on first quantization approaches and certain algebraic details are left for the Appendixes. We therefore organize the paper as follows. In Sec. II we discuss a hypothetical paired crystalline phase with electrons of *definite spin* and arranged in

an antiferromagnetic configuration; we show that there exists a paired structure (Pa3) where intercell exchange effects can be several orders of magnitude more important than the estimate based on the usual monatomic structures, and where the corresponding energy lowering can overcome the small electrostatic difference compared with the conventional bcc discussed earlier. In Sec. III we discuss paired crystalline phases where spin singlets are formed within each pair, and where the combination of intra- and intercell exchange leads to energy lowering even at the level of orientationally averaged phases (as in the orientationally averaged $\langle \text{Pa3} \rangle$ structure). Equivalently this is at the level of an effective spherical cell method,¹ but in either view it is sufficient to lead to a preference over monatomic phases. Such a phase of localized spin-singlet pairs has coherence properties of the type of a supersolid (with interconnected off-diagonal and diagonal long-range order), and we show that if these persist at higher densities and even beyond melting, they evolve into a diffusive paired phase such as the one appearing in the standard pairing theory of superconductivity. The paper concludes with a discussion of the results (Sec. IV).

II. PHASES WITH DEFINITE SPINS

Consider a three-dimensional (3D) system of N electrons in a rigid uniform compensating background. To fully account for the fermionic character we write the Hamiltonian (1) in standard second quantized form, namely

$$H = \sum_{\mathbf{k},s} \frac{\hbar^2 k^2}{2m} c_{\mathbf{k},s}^\dagger c_{\mathbf{k},s} + \frac{1}{2} \sum_{s,s'} \sum_{\mathbf{q}} \sum_{\mathbf{k}' \neq \mathbf{k}} \frac{4\pi e^2}{V|\mathbf{k}-\mathbf{k}'|} c_{\mathbf{k}'+\mathbf{q}/2,s}^\dagger c_{-\mathbf{k}'+\mathbf{q}/2,s'} \times c_{-\mathbf{k}+\mathbf{q}/2,s'} c_{\mathbf{k}+\mathbf{q}/2,s} \quad (5)$$

A general state of the system at zero temperature can be written as

$$|\Psi\rangle = \sum_{s_1, \dots, s_N} \int d^3 r_1 \cdots d^3 r_N F(\mathbf{r}_1 s_1, \dots, \mathbf{r}_N s_N) \times \psi_{s_1}^\dagger(\mathbf{r}_1) \cdots \psi_{s_N}^\dagger(\mathbf{r}_N) |0\rangle, \quad (6)$$

which can be used as a trial state in a variational evaluation of the ground-state energy. Let us first consider the choice

$$F(\mathbf{r}_1 s_1, \dots, \mathbf{r}_N s_N) = \prod_{i=1}^N f_i(\mathbf{r}_i, s_i) \quad (7)$$

with $f(\mathbf{r}_i, s_i) = f(\mathbf{r}_i - \mathbf{R}_i) \delta_{s_i, \sigma_i}$, which has been used recently¹¹ to describe a monatomic crystalline state with definite spins σ_i on sites \mathbf{R}_i . Here, however, we will use it to describe a more general state, which can be monatomic or paired, or indeed any other more complex structure, but always chosen such that each particle (i) is associated with a *definite* value of spin (σ_i). The many-electron wave function $|\Psi\rangle$ can then be rewritten as

$$|\Psi\rangle = d_{s_1}^\dagger(\mathbf{R}_1) \cdots d_{s_N}^\dagger(\mathbf{R}_N)|0\rangle, \quad (8)$$

with

$$d_{s_n}^\dagger(\mathbf{R}_n) = \int d^3r \psi_{s_n}^\dagger(\mathbf{r}) f(\mathbf{r} - \mathbf{R}_n). \quad (9)$$

By using

$$\psi_s^\dagger(\mathbf{r}) = \frac{1}{\sqrt{V}} \sum_{\mathbf{k}} e^{-i\mathbf{k}\cdot\mathbf{r}} c_{\mathbf{k}s}^\dagger \quad (10)$$

we can rewrite d^\dagger as

$$d_{s_n}^\dagger(\mathbf{R}_n) = C \sum_{\mathbf{k}} e^{-i\mathbf{k}\cdot\mathbf{R}_n} f(\mathbf{k}) c_{\mathbf{k}s_n}^\dagger, \quad (11)$$

which is clearly an operator creating an electron with spin s_n localized on site \mathbf{R}_n and with a single-particle function f whose Fourier transform is $f(\mathbf{k})$. The use of identical functions $f(\mathbf{k})$ for all sites is equivalent to an Einstein picture of uncoupled oscillators. (The effect of the inclusion of intercell dynamical correlations, i.e., phonons, has been discussed above.) It is straightforward to evaluate $\langle \Psi|H|\Psi\rangle / \langle \Psi|\Psi\rangle$ for arbitrary N , although it is a difficult problem at the end to take the limit $N \rightarrow \infty$ which, particularly for a charged system in a uniform background, is absolutely necessary [for reasons of rigorous charge neutrality, formally expressed in (5)

through the $\mathbf{k}' \neq \mathbf{k}$ restriction]. In Sec. III we will invoke a type of cluster calculation, based on a finite number of particles, and because of this we will here give for comparison the results for finite and small values of N . The question of the thermodynamic limit will be properly addressed later. But if we keep overlaps S [to be defined in Eq. (16) below] only to lowest order, which is a very good approximation for the densities of interest, then the general results are the following (for details see Appendix B).

(a) For $N=2$ electrons (one localized around $\tilde{\mathbf{R}}_1$, the other around $\tilde{\mathbf{R}}_2$) with opposite spins,

$$\begin{aligned} \langle \Psi|H|\Psi\rangle &= 2T(0) + U(0,0,\mathbf{R}), \\ \langle \Psi|\Psi\rangle &= 1 \end{aligned} \quad (12)$$

with $\mathbf{R} \equiv \tilde{\mathbf{R}}_1 - \tilde{\mathbf{R}}_2$. For the above result real and symmetric normalized functions $f(\mathbf{k})$ have been used.

(b) For $N=4$ electrons in an "antiferromagnetic" configuration (i.e., spins in opposite pairs: $1\uparrow, 2\downarrow, 3\uparrow, 4\downarrow$),

$$\langle \Psi|H|\Psi\rangle = 4T(0) + \frac{1}{2} \sum_{i \neq j} U(0,0,\mathbf{R}_{ij}) + \Delta E_{\text{ex}} + O(S^4), \quad (13)$$

$$\langle \Psi|\Psi\rangle = 1 - [S(13)^2 + S(24)^2] + O(S^4), \quad (14)$$

with

$$\begin{aligned} \Delta E_{\text{ex}} &= -2[T(13)S(13) + T(24)S(24)] - [U(13,31,13) + U(24,42,24)] \\ &\quad - 2T(0)[S(13)^2 + S(24)^2] - [U(0,0,13)S(24)^2 + U(0,0,24)S(13)^2] \\ &\quad - [U(13,0,12)S(13) + U(13,0,14)S(13) + U(24,0,23)S(24) + U(31,0,34)S(13) \\ &\quad + U(0,24,12)S(24) + U(0,42,14)S(24) + U(0,31,23)S(13) + U(0,42,34)S(24)]. \end{aligned} \quad (15)$$

(c) For arbitrary N in an antiferromagnetic configuration the results are a generalization of (13)–(15) and are given in Appendix B [Eqs. (B4)–(B6)].

In the above the three types of quantities S , T , and U are defined by

$$S(ij) \equiv S(\mathbf{R}_{ij}) = \int d^3k f(\mathbf{k})^2 e^{-i\mathbf{k}\cdot\mathbf{R}_{ij}} \quad (16)$$

the overlaps,

$$T(ij) \equiv T(\mathbf{R}_{ij}) = \int d^3k \frac{\hbar^2 k^2}{2m} f(\mathbf{k})^2 e^{-i\mathbf{k}\cdot\mathbf{R}_{ij}} \quad (17)$$

the kinetic-energy matrix elements, and

$$U(kl, mn, ij) \equiv U(\mathbf{R}_{kl}, \mathbf{R}_{mn}, \mathbf{R}_{ij}) = \sum_{\mathbf{q} \neq 0} \frac{4\pi e^2}{Vq^2} e^{i\mathbf{q}\cdot\mathbf{R}_{ij}} \int d^3k d^3k' f(\mathbf{k}+\mathbf{q}) f(\mathbf{k}-\mathbf{q}) f(\mathbf{k}) f(\mathbf{k}') e^{-i\mathbf{k}\cdot\mathbf{R}_{kl}} e^{-i\mathbf{k}'\cdot\mathbf{R}_{mn}} \quad (18)$$

the potential-energy matrix elements.

These results immediately show that exchange has an effect of lowering the energy, as anticipated, but *only* from overlaps between *parallel* spins. For example, in case (a) where we only have opposite spins, exchange has no effect on the energy at all, and we merely obtain the result expected for distinguishable particles. In all other cases (i.e., $N > 2$) the exchange lowering contains overlaps $[S(ij)]$ between sites with parallel spins *only*, i.e., in case (b) only $S(13)$ and $S(24)$ appear and never other possibilities, such as $S(12)$ or $S(34)$, etc. This result is general for any structure provided the spins are definite;

it suggests that for paired structures with opposite spins in each cell, the exchange lowering can only be of an interpair and never of an intrapair nature. Let us now apply this conclusion on the parallel-spin exchange lowering to a comparison of a Bravais lattice with a possible paired structure. The conventional bcc monatomic structure (which in the absence of exchange is lowest in energy) is also in an antiferromagnetic configuration. Thus, parallel spins, being *next* neighbors, are very far from each other and we therefore expect exchange effects from these to be negligible. This is indeed the case and it is in agreement with the conclusions drawn by Carr,⁸ who in

an approximate way estimated exchange to have a negligible and in fact exponentially small dependence on the density for a Bravais lattice.

If, however, we consider a paired structure with Pa3 as a specific example, with the spins belonging to a pair being antiparallel, and with a value of $d \simeq 0.27a$ to optimize the Madelung energy, then as noted above we find that the interpair distance between *parallel spins* can actually be smaller than the intrapair distance, and certainly smaller than the corresponding distance in the bcc antiferromagnetic phase for the same density. Because S is essentially the overlap of Gaussian functions it rises *very* rapidly with declining separation. In more detail, since the exchange energy gain in (13) is proportional to $S(R)^2$, we can estimate the exchange lowering by simply looking at the minimal distance R_{ss} between parallel spins. For bcc we have $R_{ss} = \bar{a} = 2.03098r_s a_0$ [see Fig. 1(c)] so that for a Gaussian choice [see result (51) below, which turns out to be consistent with Carr's result] and with Wigner's value of the halfwidth $\sigma = r_s^{3/4} a_0$ [see (A30)], we obtain for $r_s = 100$, the value $S^2 = 1.1 \times 10^{-9}$. For the Pa3 structure [see Fig. 1(b)], however, we have $R_{ss} = BC = 1.72375r_s a_0$ and accordingly, for the same choice of Gaussian function, we obtain $S^2 = 3.5 \times 10^{-7}$, i.e., already two orders of magnitude higher. In addition, if we allow for σ itself to be larger, we can actually increase the magnitude of the effect by yet another three orders of magnitude. For example, if we use $\sigma = 43a_0$ (the resulting *optimal* value for $r_s = 100$ as will be found in Sec. III; see Fig. 2) we obtain $S^2 = 3.2 \times 10^{-4}$, which corresponds to five orders of magnitude higher energy gain than the previous estimate for the conventional monatomic case. Allowing for coordination these energy gains are of order of 3/100 mRy, as we will now see in detail. (We will see in Sec. III, where we allow for the possibility of singlet resonance between the opposite spins of a pair and include intrapair exchange as well, that the energy gain is even larger, rising to 2/10 mRy).

What this indicates is that the effect of parallel spin exchange, which certainly operates in the conventional Wigner crystal, but to a quite negligible degree at low densities, can be several orders of magnitude stronger in paired phases. This is a key difference in the exchange contribution between conventional monatomic and paired structures. We can give an actual estimate of the exchange lowering for the Pa3 structure [in the case of Gaussian choices we use Eqs. (51)–(58) below], based on a cluster consisting of a central pair and the 12 neighboring pairs at the actual positions for the Pa3 structure [see Fig. 4(b)], and again with the optimal value $d = 0.27a$. Using the result (13)–(15) for the exchange energy gain per neighboring pair, we obtain an energy lowering

$$\epsilon = \frac{\epsilon_{\text{Pa3}} + \frac{12}{26} \Delta E_{\text{ex}}}{1 - 12[S(13)^2 + S(24)^2]} - \epsilon_{\text{Pa3}}$$

per electron. For the choices $r_s = 100$ and $\sigma = 43a_0$ (the optimal values found in Sec. III) this gives $\epsilon = -8.317 \times 10^{-2}$ mRy, which is to be contrasted with the electrostatic penalty $\epsilon_{\text{Pa3}} - \epsilon_{\text{bcc}} = 5.590 \times 10^{-2}$ mRy per electron. Even for r_s as high as 150 (and the corresponding value $\sigma = 63a_0$) we obtain $\epsilon = -3.770 \times 10^{-2}$

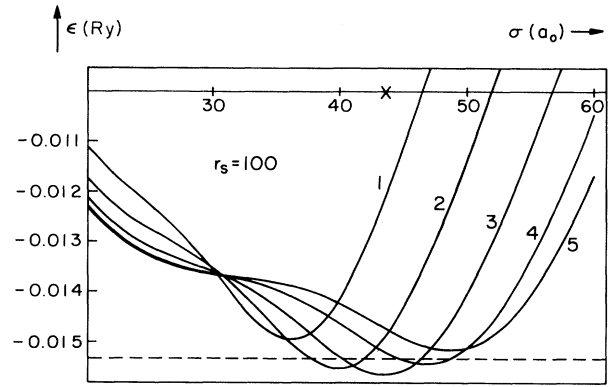


FIG. 2. Typical minimization procedure for $r_s = 100$ of the ground-state energy per electron with respect to the pair size R and the half width σ of each Heitler-London Gaussian orbital. Curve 1 corresponds to $R = 90a_0$; curve 2 to $R = 100a_0$; curve 3 to $R = 110a_0$; curve 4 to $R = 120a_0$; and curve 5 to $R = r_{\text{WS}} = 2^{1/3}r_s a_0 \sim 126a_0$. Curve 3 gives the optimal values $R_0 = 110a_0$ and $\sigma_0 = 43a_0$. Dashed line: Wigner crystal (Ref. 14).

mRy, which is to be compared with $\epsilon_{\text{Pa3}} - \epsilon_{\text{bcc}} = 3.727 \times 10^{-2}$ mRy. We therefore conclude that exchange lowering in the Pa3 structure is by itself sufficient to overcome the electrostatic penalty, provided that the density is not too low (see also Sec. IV and Fig. 3). This

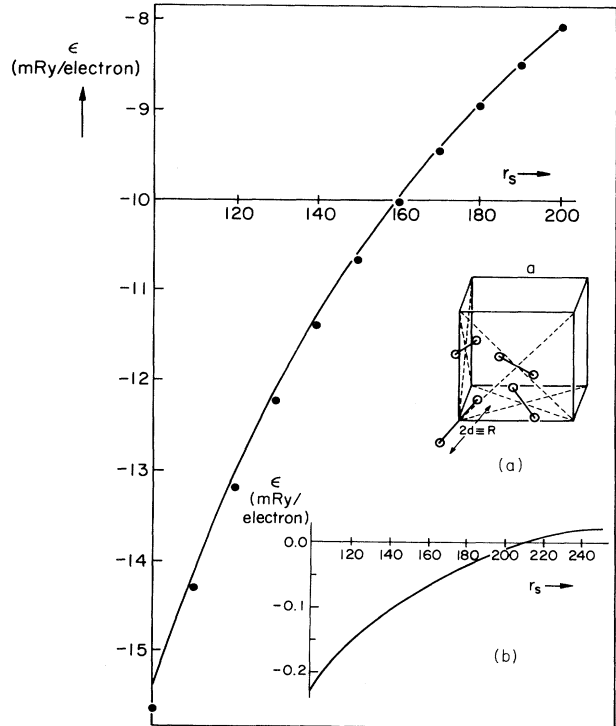


FIG. 3. Ground-state energy per electron as a function of density. Dots, the paired electron supersolid for the (Pa3) structure; solid curve, the conventional monatomic Wigner crystal (Ref. 14). Inset (a): Pa3 structure. Inset (b): the difference between the paired crystal energy/electron and the Wigner crystal energy/electron as a function of density.

pairing, as discussed earlier, can be viewed as an exchange induced 3D Peierls transition starting from a Bravais (simple cubic) lattice.

III. PHASES OF PAIRED SINGLETs

We now consider an alternative choice of trial state, namely a crystalline structure of spin-singlet pairs of electrons. The two electrons participating in each pair no longer have definite spins; instead they resonate between the two possible combinations of antiparallel spins in a completely spin-antisymmetric fashion (i.e., $|\uparrow\downarrow\rangle - |\downarrow\uparrow\rangle$). This phase is described by the choice

$$F(\mathbf{r}_1 s_1, \dots, \mathbf{r}_N s_N) = \prod_{l(i,j)} f_{ij}^l(\mathbf{r}_i, \mathbf{r}_j) \delta_{s_i, -s_j} \quad (19)$$

with f_{ij}^l constrained to be symmetric under interchange of \mathbf{r}_i and \mathbf{r}_j and where the product is over distinct pairs belonging to a site labeled by l . The corresponding trial state can be written as

$$|\Psi\rangle = d_{1,2}^\dagger(\mathbf{R}_1) d_{3,4}^\dagger(\mathbf{R}_2) \cdots d_{N-1,N}^\dagger(\mathbf{R}_{N/2}) |0\rangle \quad (20)$$

with

$$d_{i,j}^\dagger(\mathbf{R}_l) = \int d^3 r_i d^3 r_j f_{ij}^l(\mathbf{r}_i, \mathbf{r}_j) \psi_\uparrow^\dagger(\mathbf{r}_i) \psi_\downarrow^\dagger(\mathbf{r}_j), \quad (21)$$

which may be compared with (9) for the choice made in a phase with definite spins. By using (10) and the separation of the pair state into a center of mass and internal wave function, namely

$$f_{ij}^l(\mathbf{r}_i, \mathbf{r}_j) = \Phi^l \left[\frac{\mathbf{r}_i + \mathbf{r}_j}{2} \right] \phi(\mathbf{r}_i, \mathbf{r}_j), \quad (22)$$

the operator $d_{i,j}^\dagger(\mathbf{R}_l)$ creating a pair (i,j) with center of mass \mathbf{R}_l can also be written as

$$d_{i,j}^\dagger(\mathbf{R}_l) = C \sum_{\mathbf{q}} e^{-i\mathbf{q}\cdot\mathbf{R}_l} \Phi(\mathbf{q}) \times \sum_{\mathbf{k}} \phi^{(i,j)}(\mathbf{k}) c_{\mathbf{k}+(\mathbf{q}/2)\uparrow}^\dagger c_{-\mathbf{k}+(\mathbf{q}/2)\downarrow}^\dagger, \quad (23)$$

where the spatial internal wave function is required to be symmetric for spin-singlet states, i.e., $\phi^{(i,j)}(-\mathbf{k}) = \phi^{(i,j)}(\mathbf{k}) = \phi^{(j,i)}(\mathbf{k})$. Here Φ is the center-of-mass wave function of each pair which, in an Einstein oscillator picture, is identical for all pairs. Correspondingly $\phi^{(i,j)}$ is the internal wave function of pair (i,j) .

Not surprisingly, the evaluation of $\langle \Psi | H | \Psi \rangle / \langle \Psi | \Psi \rangle$ is considerably more complicated than the case for definite spins. It will be facilitated later when we write the paired states (i,j) in each site l as a Heitler-London combination of two single-particle states. For the moment, however, we retain a more general approach in order to establish a formal device that will prove extremely useful in what follows.

Consider therefore (20) as a trial state of N electrons, forming $N/2$ spin-singlet pairs, with the pair operators d^\dagger given by (23). The center-of-mass wave function $\Phi(\mathbf{q})$ can be taken as Gaussian [in the form $\Phi(\mathbf{q}) \sim e^{-\sigma^2 q^2/4}$, as we shall see below in Eq. (32), σ being proportional to the width of the Gaussian in r space] for the ground state in

the Einstein oscillator picture. A consideration of two special limiting cases will be helpful in what follows: (i) extreme localization corresponding to the choice $\sigma \rightarrow 0$, or equivalently to the choice $\Phi(\mathbf{q}) = \text{const}$; (ii) extreme delocalization (diffusive pairs) corresponding to the choice $\sigma \rightarrow \infty$, or better to the choice $\Phi(\mathbf{q}) \sim \delta(\mathbf{q})$.

Case (ii) immediately gives

$$|\Psi\rangle = \left(\sum_{\mathbf{k}} \phi(\mathbf{k}) c_{\mathbf{k}\uparrow}^\dagger c_{-\mathbf{k}\downarrow}^\dagger \right)^{N/2} |0\rangle \quad (24)$$

where for this diffusive case ϕ is taken the same for all (i,j) 's, since the pairs have maximal overlap and the labels l or (i,j) do not matter. In the limit $N \rightarrow \infty$ this leads to the standard pairing theory (to Cooper or Schafroth pairs) of superconductivity, as we discuss below. The above description [based on (20)] therefore contains *both* limits of extremely localized and of extremely delocalized pairs and we can go from one to the other "smoothly" by changing the parameter σ . However, we are most concerned with the case of intermediate values of σ (i.e., we will keep the Gaussian function in general form), and although our results will apply to a phase of localized pairs, the localization will *not* be extreme. In fact σ will have a finite and nonvanishing value, dependent on the density, which will be determined variationally.

A. Diffusive case

We first treat the extremely delocalized case [$\Phi(\mathbf{q}) \sim \delta(\mathbf{q})$] in order to establish a very useful recursive method that can later be used in the general case to determine the ground-state energy. In this diffusive case the trial state is given by (24), which we can call $|N/2\rangle$. To evaluate

$$\frac{\left\langle \frac{N}{2} \left| H \right| \frac{N}{2} \right\rangle}{\left\langle \frac{N}{2} \left| \frac{N}{2} \right\rangle \right.}$$

in the limit $N \rightarrow \infty$, we apply a recursive procedure¹² published earlier: it is quite straightforward to write the matrix elements $\langle N/2 | c^\dagger c | N/2 \rangle$ and $\langle N/2 | c^\dagger c^\dagger c c | N/2 \rangle$ exactly in terms of the corresponding elements $\langle N/2-1 | c^\dagger c | N/2-1 \rangle$ and $\langle N/2-1 | c^\dagger c^\dagger c c | N/2-1 \rangle$ with respect to (24), but with N replaced by $N-2$, i.e., a state with one pair less. The crucial step is that at the end we set corresponding elements (differing by one pair) equal to each other in the limit $N \rightarrow \infty$, acknowledging thereby the fact that in the thermodynamic limit removal of one pair essentially leaves all the physical properties of the state unchanged. This strategy is a canonical method for determining the BCS gap equation and when applied here immediately gives the following results: (a) For the one-body elements,

$$\langle c_{\mathbf{k}\uparrow}^\dagger c_{\mathbf{k}\uparrow} \rangle = \frac{\lambda^2 |\phi(\mathbf{k})|^2}{1 + \lambda^2 |\phi(\mathbf{k})|^2} \quad (25)$$

and (b) for the two-body elements, and for $\mathbf{k}' \neq \mathbf{k}$ [which is required from the restriction in (5)],

$$(i) \langle c_{\mathbf{k}'+\mathbf{q}/2,s}^\dagger c_{-\mathbf{k}'+\mathbf{q}/2,-s}^\dagger c_{-\mathbf{k}+\mathbf{q}/2,-s} c_{\mathbf{k}+\mathbf{q}/2,s} \rangle = \begin{cases} 0 & \text{for } \mathbf{q} \neq 0 \\ \frac{\lambda \phi^*(\mathbf{k}') \lambda \phi(\mathbf{k})}{[1 + \lambda^2 |\phi(\mathbf{k})|^2][1 + \lambda^2 |\phi(\mathbf{k}')|^2]} & \text{for } \mathbf{q} = 0 \end{cases} \quad (26)$$

for the *antiparallel* spin correlations and

$$(ii) \langle c_{\mathbf{k}'+\mathbf{q}/2,s}^\dagger c_{-\mathbf{k}'+\mathbf{q}/2,s}^\dagger c_{-\mathbf{k}+\mathbf{q}/2,s} c_{\mathbf{k}+\mathbf{q}/2,s} \rangle = \begin{cases} 0 & \text{for } \mathbf{k}' \neq -\mathbf{k}, \\ \frac{-\lambda^2 \left| \phi \left[\mathbf{k} + \frac{\mathbf{q}}{2} \right] \right|^2 \left| \phi \left[\mathbf{k} - \frac{\mathbf{q}}{2} \right] \right|^2}{\left[1 + \lambda^2 \left| \phi \left[\mathbf{k} + \frac{\mathbf{q}}{2} \right] \right|^2 \right] \left[1 + \lambda^2 \left| \phi \left[\mathbf{k} - \frac{\mathbf{q}}{2} \right] \right|^2 \right]} & \text{for } \mathbf{k}' = -\mathbf{k} \end{cases} \quad (27)$$

for the *parallel* spin correlations. The normalization constant λ is self-consistently determined through fixing the number of particles. As noted above these results give¹² the standard pairing theory of superconductivity at intermediate densities [where the antiparallel spin correlations (26) are dominant] and also the normal Hartree-Fock theory in the asymptotic high-density limit [where now the parallel spin correlations (27) become dominant].

It is important to recognize that the results (25)–(27) lead to modifications of both kinetic and potential energies [i.e., the expectation value of the first and second terms of (5)] relative to the normal Hartree-Fock limit, and these arise from the effects of exchange (or better, the imposition from the very beginning of the antisymmetry of the total wave function). This modification, for example, plays a crucial role in the fact that a superconducting state has an energy lower than the normal (unpaired diffusive) state. A major result of this paper will be that a similar source of energy lowering will *also* be found in the localized pair case, and although it is small (as expected for a solid), it will still be crucial in lowering the energy below that of a monatomic (unpaired) solid at least in a certain range of densities. In this sense, were the monatomic solid to be viewed as the “analog” of the normal state, then a paired crystal would be viewed as the analog of the superconducting state. This viewpoint can offer a generalization of the concept of a supersolid (one consisting of localized neutral bosons that have proceeded through Bose condensation, as treated by Chester⁷) to a paired supersolid (one consisting of localized charged paired fermions, but in a type of superconducting condensation, where the internal structure now plays a crucial role).

What is of particular interest here, however, is the formal *low-density* limit of Eqs. (25)–(27). An expansion of the above results (of the thermodynamic system) with respect to the constant λ^2 is now very useful: the lowest-order form for $\langle H \rangle$ has the structure of the result one obtains from consideration of, and exact solution of, but a *single* (diffusive) pair. Inclusion of the next-order correction also reproduces the structure of the exact solution, but for a system consisting of *two* pairs, and so on. We see therefore that correlations in the thermodynamic system propagate through a “one-dimensional path” con-

sisting just of the number of pairs; this should be expected for a case where the pairs are maximally overlapping and where their centers of mass all have equal probability of being anywhere in space.

A similar observation can be made for the general case of finite width σ , i.e., for pairs with their centers of mass localized on lattice sites [but where now the labels l and (i, j) are distinct]. In this case we shall show that once again an expansion with respect to some constant, analogous to λ^2 (which is again fixed by normalization), is very useful: the lowest-order result has the structure of a *single* pair, but now localized around a center. We shall also argue that inclusion of the next-order result gives the structure of the result for a close-packed *cluster* consisting of a central pair, taken together with all n neighboring pairs that cover it symmetrically (n depending on the structure), i.e., just the result of a system with $2(n+1)$ electrons. (We will later take $n=12$ having in mind a Pa3 structure.) This picture is expected from the localization property and the consequent existence of the lattice site labels, which makes the above $2(n+1)$ -electron system to be the “minimal” problem to be solved for the determination of the effect of interpair exchange in a paired crystal phase. It shows that correlations in the crystal now propagate not merely through a one-dimensional path but through a “three-dimensional path,” which is the cluster under consideration. But of course *any* pair, even the one used initially as a neighboring pair, can be used as a central choice in a new cluster, and in this way correlations again propagate through the entire system. We will use these observations in what follows, together with the imposition of a self-consistency, namely that any of the n neighboring pairs must be equivalent to the central pair in order to evaluate the ground-state energy of the above localized paired phase in a variant of the Bethe method of improving mean-field estimates in problems involving magnetic order.

B. Localized case (the paired crystal)

1. Pairing ($\Phi - \phi$) description

We begin by working to lowest order in density. It can be easily shown that the result to this order is the same as

the result for a single pair with its center of mass vibrating around, say \mathbf{R}_1 . The evaluation of the ground-state energy in terms of the pairing description (20) is straightforward and gives the following results.

For the state (20), but written as

$$|\Psi\rangle = d_{1,2}^\dagger(\mathbf{R}_1)|\psi_3 \cdots N\rangle, \quad (28)$$

with d^\dagger given by (23), we obtain, exactly

$$\langle \Psi | c_{\mathbf{k},s}^\dagger c_{\mathbf{k},s} | \Psi \rangle = |C|^2 \sum_{\mathbf{q}} |\Phi(\mathbf{q})|^2 \left| \phi^{(1,2)} \left[\mathbf{k} - \frac{\mathbf{q}}{2} \right] \right|^2 + O(|C|^4), \quad (29)$$

$$\langle \Psi | c_{\mathbf{k}'+\mathbf{q}/2, \uparrow}^\dagger c_{-\mathbf{k}'+\mathbf{q}/2, \uparrow}^\dagger c_{-\mathbf{k}+\mathbf{q}/2, \uparrow}^\dagger c_{\mathbf{k}+\mathbf{q}/2, \uparrow} | \Psi \rangle = |C|^2 |\Phi(\mathbf{q})|^2 \phi^{(1,2)}(\mathbf{k}')^* \phi^{(1,2)}(\mathbf{k}) + O(|C|^4), \quad (30)$$

and

$$\langle \Psi | c_{\mathbf{k}'+\mathbf{q}/2, \uparrow}^\dagger c_{-\mathbf{k}'+\mathbf{q}/2, \uparrow}^\dagger c_{-\mathbf{k}+\mathbf{q}/2, \uparrow}^\dagger c_{\mathbf{k}+\mathbf{q}/2, \uparrow} | \Psi \rangle = -|C|^3 |\Phi(\mathbf{q})|^2 |\phi^{(1,2)}(\mathbf{k}')|^2 |\phi^{(1,2)}(\mathbf{k})|^2 + O(|C|^4), \quad (31)$$

which are also the results that we would have obtained for $N=2$ (or equivalently by setting $|\psi_3 \cdots N\rangle \equiv |0\rangle$), as discussed earlier. The constant $|C|^2$ is determined by self-consistently fixing the number of particles [see (36) and (37) below].

We may simplify matters by making the following choices of wave functions, namely

$$\Phi(\mathbf{q}) = \frac{1}{\sqrt{V}} (2\pi\sigma^2)^{3/4} e^{-\sigma^2 \mathbf{q}^2/4} \quad (32)$$

and

$$\phi^{(1,2)}(\mathbf{k}) = \frac{1}{\sqrt{V}} (8\pi\sigma^2)^{3/4} e^{-k^2\sigma^2} \cos \mathbf{k} \cdot \mathbf{R}. \quad (33)$$

Both are "normalized," according to $\sum_{\mathbf{q}} |\Phi(\mathbf{q})|^2 = 1$ for the center-of-mass wave function, and $\sum_{\mathbf{k}} |\phi(\mathbf{k})|^2 = [1+S(R)^2]/2$ for the internal wave function. We adopt as a definition $S(R) = e^{-R^2/4\sigma^2}$. For the moment \mathbf{R} is an arbitrary vector, but we will see below that these choices actually correspond to the Heitler-London com-

ination of two single-particle states of Gaussian form, one centered about $\tilde{\mathbf{R}}_1$ and the other about $\tilde{\mathbf{R}}_2$, provided that we take $\mathbf{R} \equiv \tilde{\mathbf{R}}_1 - \tilde{\mathbf{R}}_2$. For these choices the pair (1,2) has center of mass vibrating around $(\tilde{\mathbf{R}}_1 + \tilde{\mathbf{R}}_2)/2$, and therefore we must also impose $\mathbf{R}_1 = (\tilde{\mathbf{R}}_1 + \tilde{\mathbf{R}}_2)/2$. These conditions fix $\tilde{\mathbf{R}}_1$ and $\tilde{\mathbf{R}}_2$ in terms of \mathbf{R}_1 and \mathbf{R} . In addition, we will see that $S(R)$ as defined above will be the overlap integral between the two single-particle Gaussian functions.

With these choices we find

$$\langle \Psi | c_{\mathbf{k},s}^\dagger c_{\mathbf{k},s} | \Psi \rangle = |C|^2 \frac{4\pi^{3/2}}{V} \sigma^3 e^{-k^2\sigma^2} (1 + e^{-R^2/4\sigma^2} \cos \mathbf{k} \cdot \mathbf{R}), \quad (34)$$

which is a quite interesting form for the occupation number of the free-particle state (\mathbf{k}, s) . The corresponding kinetic energy is

$$\langle T \rangle = \sum_s \sum_{\mathbf{k}} \frac{\hbar^2 k^2}{2m} \langle \Psi | c_{\mathbf{k},s}^\dagger c_{\mathbf{k},s} | \Psi \rangle = |C|^2 \frac{3a_0^2}{2\sigma^2} \left[1 + e^{-R^2/2\sigma^2} - \frac{R^2}{6\sigma^2} e^{-R^2/2\sigma^2} \right] \text{Ry}. \quad (35)$$

As noted above the constant $|C|^2$ is determined by self-consistency, namely,

$$\sum_s \sum_{\mathbf{k}} \langle \Psi | c_{\mathbf{k},s}^\dagger c_{\mathbf{k},s} | \Psi \rangle = N, \quad (36)$$

which, with the above choices of Φ and ϕ , finally gives

$$|C|^2 = \frac{N}{1 + e^{-R^2/2\sigma^2}}. \quad (37)$$

Hence we find

$$\langle T \rangle = \frac{N}{1+S(R)^2} \left[\frac{3}{2} \frac{a_0^2}{\sigma^2} + \frac{3}{2} \frac{a_0^2}{\sigma^2} S(R)^2 \left[1 - \frac{R^2}{6\sigma^2} \right] \right] \text{Ry}. \quad (38)$$

Finally the potential energy in the same approximation is

$$\langle U \rangle = \sum_{\mathbf{q}} \sum_{\mathbf{k} \neq \mathbf{k}'} \frac{4\pi e^2}{V |\mathbf{k} - \mathbf{k}'|^2} \left[\langle \Psi | c_{\mathbf{k}'+\mathbf{q}/2, \uparrow}^\dagger c_{-\mathbf{k}'+\mathbf{q}/2, \uparrow}^\dagger c_{-\mathbf{k}+\mathbf{q}/2, \downarrow}^\dagger c_{\mathbf{k}+\mathbf{q}/2, \uparrow} | \Psi \rangle + \langle \Psi | c_{\mathbf{k}'+\mathbf{q}/2, \uparrow}^\dagger c_{-\mathbf{k}'+\mathbf{q}/2, \uparrow}^\dagger c_{-\mathbf{k}+\mathbf{q}/2, \uparrow}^\dagger c_{\mathbf{k}+\mathbf{q}/2, \uparrow} | \Psi \rangle \right], \quad (39)$$

which using (30) and (31) and the choices (32) and (33) gives for the first term in (39)

$$\langle U \rangle_{\uparrow\downarrow} = |C|^2 \sum_{\mathbf{K} \neq 0} \frac{4\pi e^2}{VK^2} \sum_{\mathbf{q}} |\Phi(\mathbf{q})|^2 \sum_{\mathbf{k}} \phi^*(\mathbf{k} + \mathbf{K}) \phi(\mathbf{k}) = |C|^2 \frac{1}{2} \sum_{\mathbf{K} \neq 0} \frac{4\pi e^2}{VK^2} e^{-K^2\sigma^2/2} (e^{-R^2/2\sigma^2} + \cos \mathbf{K} \cdot \mathbf{R}) \quad (40)$$

as the contribution from antiparallel spins. If for the moment we ignore the neutrality $\mathbf{K} \neq 0$ restriction, this will give

$$\frac{|C|^2}{2} \left[2\sqrt{2/\pi} \frac{a_0}{\sigma} e^{-R^2/2\sigma^2} + \frac{2a_0}{R} \text{erf} \left[\frac{R}{\sqrt{2}\sigma} \right] \right] \text{Ry}. \quad (41)$$

The second term in (39) (the contribution from parallel spins) is proportional to $-(|C|^3/V)\sigma^3$ and hence to (density) $\times \sigma^3 \times N^{1/2}$; accordingly this term divided by N will give a vanishing contribution per particle in the limit $N \rightarrow \infty$. This should actually be expected from the consideration of a single pair where there are in any case no parallel spins in a singlet state; the contribution of this second term is an exchange lowering which is of a *normal* character, i.e., it is the dominant contribution only in the extremely high-density limit where it turns out to be equal to the usual Hartree-Fock exchange in the diffusive limit. But it gives zero contribution in the low-density limit we are considering here and the final result, again without accounting for the neutrality $\mathbf{K} \neq 0$ restriction, is

$$\langle U \rangle = \frac{N}{1+S(R)^2} \frac{1}{2} \left[\frac{2a_0}{R} \operatorname{erf} \left[\frac{R}{\sqrt{2}\sigma} \right] + 2\sqrt{2/\pi} \frac{a_0}{\sigma} S(R)^2 \right] R y. \quad (42)$$

The contribution from the $\mathbf{K} = 0$ term will be discussed later, when the presence of the neutralizing background will be properly taken into account in the thermodynamic limit.

These results are the lowest-order results in $|C|^2$ and represent the lowest contribution valid in the zero-density limit (they give exactly the same result as for a single pair, i.e., if we set $N=2$, they also agree with the results of Appendix A, where a simpler first quantization approach is followed). It is clear then that they contain the effect of pure *intrapair* exchange only. If we now want to go further to examine the *interpair* contribution, we must proceed to the next nontrivial order in $|C|^2$, which is actually of $O(|C|^2)^{n+1}$ because of the consequences of localization and the corresponding existence of $n+1$ distinct labels, as discussed earlier. To do this it is more convenient to change language, as follows.

2. Heitler-London description

A major simplification in the algebraic treatment of the localized paired state ensues if we assume a Heitler-London form of single-particle functions for the pair function $f_{ij}^l(\mathbf{r}_i, \mathbf{r}_j)$ of (19). Accordingly, we now write

$$f_{ij}^l(\mathbf{r}_i, \mathbf{r}_j) = (\text{const}) [f(\mathbf{r}_i - \tilde{\mathbf{R}}_i) f(\mathbf{r}_j - \tilde{\mathbf{R}}_j) + f(\mathbf{r}_i - \tilde{\mathbf{R}}_j) f(\mathbf{r}_j - \tilde{\mathbf{R}}_i)] \quad (43)$$

[rather than (22)], which describes a spin-singlet pair state in each cell, again in an Einstein picture. It may be viewed, of course, as a variational state. Then the pair operator (21) now reads

$$d_{i,j}^\dagger(\mathbf{R}_i) = d^\dagger(\tilde{\mathbf{R}}_i) d^\dagger(\tilde{\mathbf{R}}_j) + d^\dagger(\tilde{\mathbf{R}}_j) d^\dagger(\tilde{\mathbf{R}}_i) \quad (44)$$

instead of (23), where $\mathbf{R}_i = (\tilde{\mathbf{R}}_i + \tilde{\mathbf{R}}_j)/2$, as expected. Here the single-particle operators are given by (11) and are the same operators that have been used previously in the treatment of monatomic (Wigner) crystals or, more generally, in structures with definite spin, as discussed in

Sec. II.

This connection between the pair operators (21) and the single-particle operators (9) is an important one because the same algebraic treatment used for phases with definite spin (Sec. II) can now also be used for paired phases but with spin-singlet pairs. The trial state (20) is written as

$$\begin{aligned} |\Psi\rangle = & [d^\dagger(\tilde{\mathbf{R}}_1) d^\dagger(\tilde{\mathbf{R}}_2) + d^\dagger(\tilde{\mathbf{R}}_2) d^\dagger(\tilde{\mathbf{R}}_1)] \\ & \times [d^\dagger(\tilde{\mathbf{R}}_3) d^\dagger(\tilde{\mathbf{R}}_4) + d^\dagger(\tilde{\mathbf{R}}_4) d^\dagger(\tilde{\mathbf{R}}_3)] \times \cdots \\ & \times [d^\dagger(\tilde{\mathbf{R}}_{N-1}) d^\dagger(\tilde{\mathbf{R}}_N) + d^\dagger(\tilde{\mathbf{R}}_N) d^\dagger(\tilde{\mathbf{R}}_{N-1})] |0\rangle, \end{aligned} \quad (45)$$

which should be compared with a phase with definite spins, for example, a Wigner or paired crystal in an anti-ferromagnetic configuration, namely

$$|\mathcal{W}\rangle = d^\dagger(\mathbf{R}_1) d^\dagger(\mathbf{R}_2) \cdots d^\dagger(\mathbf{R}_{N-1}) d^\dagger(\mathbf{R}_N) |0\rangle, \quad (46)$$

as used in Sec. II [see (8)]. The evaluation of $\langle \mathcal{W} | H | \mathcal{W} \rangle / \langle \mathcal{W} | \mathcal{W} \rangle$ has actually been carried out by van Dijk and Vertogen¹¹ and is reviewed in Appendix B. The evaluation of $\langle \Psi | H | \Psi \rangle / \langle \Psi | \Psi \rangle$, for the case of spin-singlet resonances within distinct pairs, is more complicated because of the need to include all possible types of interference terms that result from the form of (45). The consequence of these interference terms is the fact that, *not only* overlaps between parallel spins contribute [as for the case of (46) discussed in Sec. II], but indeed *all* combinations of overlaps contribute to the exchange effect on the energy. Consequently we will see that a combinations of overlaps contribute to the exchange effect on the energy. Consequently we will see that a combination of intrapair *and* interpair exchange effects will lower the energy even further than in the fixed spin case discussed in Sec. II. The evaluation of the ground-state energy is discussed in Appendix B. Here we again only give the final results.

$$|\Psi\rangle = [d^\dagger(\tilde{\mathbf{R}}_1) d^\dagger(\tilde{\mathbf{R}}_2) + d^\dagger(\tilde{\mathbf{R}}_2) d^\dagger(\tilde{\mathbf{R}}_1)] \psi_3 \cdots N \rangle \quad (47)$$

as in (28), we obtain the result for a single pair, which for real and symmetric $f(\mathbf{r})$ turns out to be

$$\begin{aligned} \frac{\langle \Psi | H | \Psi \rangle}{\langle \Psi | \Psi \rangle} &= \frac{2T(0) + U(0, 0, \mathbf{R}) + 2S(\mathbf{R})T(\mathbf{R}) + U(\mathbf{R}, -\mathbf{R}, \mathbf{R})}{1 + S(\mathbf{R})^2} \end{aligned} \quad (48)$$

for the energy *per pair*, with $\mathbf{R} \equiv \tilde{\mathbf{R}}_1 - \tilde{\mathbf{R}}_2$. This should be compared directly with the corresponding result (12) of Sec. II. The various elements have been defined in (16)–(18).

The result (48) contains only pure *intrapair* exchange. To make contact with the pairing description of Sec. III B 1, we again take a Gaussian choice for the single-particle functions, namely

$$f(\mathbf{r}-\mathbf{R}_i) = \frac{1}{(\pi\sigma^2)^{3/4}} e^{-(\mathbf{r}-\mathbf{R}_i)^2/2\sigma^2}, \quad (49)$$

or equivalently

$$f(\mathbf{k}) = \frac{1}{(2\pi)^{3/2}} (4\pi\sigma^2)^{3/4} e^{-\sigma^2 k^2/2}. \quad (50)$$

With such a choice the three types of matrix elements defined in (16)–(18) take the following forms:

$$S(\mathbf{R}) = e^{-R^2/4\sigma^2} \quad (51)$$

for the overlaps,

$$T(\mathbf{R}) = S(\mathbf{R}) \frac{3a_0^2}{2\sigma^2} \left[1 - \frac{R^2}{6\sigma^2} \right] \text{Ry} \quad (52)$$

for the kinetic-energy elements, and

$$U(\mathbf{R}_1, \mathbf{R}_2, \mathbf{R}) = S(\mathbf{R}_1)S(\mathbf{R}_2) \times \sum_{\mathbf{q} \neq 0} \frac{4\pi e^2}{Vq^2} e^{-q^2\sigma^2/2 + i\mathbf{q} \cdot (\mathbf{R}-\mathbf{R}_1/2 + \mathbf{R}_2/2)} \quad (53)$$

for the potential-energy elements. If for the moment we ignore the neutrality $\mathbf{q} \neq 0$ restriction, we can actually carry out the Gaussian integration in (53) and rewrite it as

$$U(\mathbf{R}_1, \mathbf{R}_2, \mathbf{R}) = \frac{2a_0}{\left| \mathbf{R} - \frac{\mathbf{R}_1}{2} + \frac{\mathbf{R}_2}{2} \right|} S(\mathbf{R}_1)S(\mathbf{R}_2) \times \text{erf} \left(\frac{\left| \mathbf{R} - \frac{\mathbf{R}_1}{2} + \frac{\mathbf{R}_2}{2} \right|}{\sqrt{2}\sigma} \right) \text{Ry}. \quad (54)$$

The above results give

$$T(0) = \frac{3a_0^2}{2\sigma^2} \text{Ry} \quad (55)$$

for the direct kinetic energy (this is equal to $\frac{3}{4}\hbar\omega$ as expected). They also give

$$T(\mathbf{R}) = S(\mathbf{R})T(0) \left[1 - \frac{R^2}{6\sigma^2} \right] \text{Ry} \quad (56)$$

for the exchange kinetic energy,

$$U(0,0,\mathbf{R}) = \frac{2a_0}{R} \text{erf} \left[\frac{R}{\sqrt{2}\sigma} \right] \text{Ry} \quad (57)$$

for the direct Coulomb repulsion [which is $(e^2/R)\text{erf}(R/\sqrt{2}\sigma)$, again as expected for smeared charges], and

$$U(\mathbf{R}, -\mathbf{R}, \mathbf{R}) = \lim_{|\mathbf{R}-\mathbf{R}_1/2+\mathbf{R}_2/2| \rightarrow 0} U(\mathbf{R}_1, \mathbf{R}_2, \mathbf{R}) = 2a_0 S(R)^2 \lim_{P \rightarrow 0} \left[\frac{\text{erf} \left[\frac{P}{\sqrt{2}\sigma} \right]}{P} \right] = S(R)^2 2\sqrt{2}/\pi \frac{a_0}{\sigma} \text{Ry} \quad (58)$$

for the exchange Coulomb repulsion. As can easily be seen, the result (48) combined with Eqs. (55)–(58) reproduces exactly the energy $\langle T \rangle + \langle U \rangle$ as given by the results (38) and (42) obtained earlier with the recursive method in $\Phi - \phi$ description for localized paired states to lowest order in density (just intrapair exchange). What remains therefore is to proceed to the next nontrivial order and to account for the interpair effect. But before proceeding, let us now discuss the $\mathbf{q} \neq 0$ restriction and the issue of neutrality.

To lowest order the above results are essentially those for a single pair ($N=2$ electrons), but with the omission of the $\mathbf{q}=0$ term from the potential energy they do *not* actually take into account the existence of the compensating background and the lattice environment (which can both be rigorously considered only in the thermodynamic limit $N \rightarrow \infty$). We can easily correct this omission by retaining the *form* of the above results (as would be expected for the full thermodynamic system in the extremely low-density limit, as discussed earlier), but by also now incorporating the background within this same form. We accomplish this in the following way.

The background gives rise to two contributions: (i) its self-energy ϵ_{bb} , which will have to be *added* to the total energy, and (ii) its electrostatic interaction with the electrons, which for a crystal and in a spherical cell approximation (discussed in Appendix A) can be represented through the standard harmonic well [see Appendix A, Eq. (A41)] as given by

$$V_b(\mathbf{r}) = -\frac{e}{2r_s^3 a_0^3} r^2 + \frac{3e}{2^{1/3} r_s a_0}. \quad (59)$$

These contributions are important parts of the Madelung energy of a paired lattice structure and they are straightforwardly determined in a spherical cell method in Appendix A. The results in the low-density limit are, *per pair*,

$$\epsilon = \epsilon_{bb} + \epsilon_{eb} + \epsilon_{ee} + \epsilon_{\text{kin}}, \quad (60)$$

$$\epsilon_{bb} = \frac{6}{5r_s} 2^{5/3} \text{Ry}, \quad (61)$$

$$\epsilon_{eb} = -\frac{3}{r_s} 2^{5/3} + \frac{3}{r_s^3} \frac{\sigma^2}{a_0^2} + \frac{1}{2r_s^3} \frac{R^2}{a_0^2} \text{Ry}, \quad (62)$$

$$\epsilon_{ee} = \frac{e^2}{R} \text{erf} \left[\frac{R}{\sqrt{2}\sigma} \right] = \frac{2a_0}{R} \text{erf} \left[\frac{R}{\sqrt{2}\sigma} \right] \text{Ry}, \quad (63)$$

and

$$\epsilon_{\text{kin}} = \frac{3}{2} \hbar\omega = 3 \frac{a_0^2}{\sigma^2} \text{Ry}. \quad (64)$$

Accordingly, in order to represent the low-density limit of the *actual* thermodynamic system we have to add ϵ_{bb} to (48), and at the same time we have to renormalize the direct element $U(0,0,\mathbf{R})$ in such a way that it gives the correct Madelung energy in (60). It is easy to see that this can be achieved by taking

$$U(0,0,\mathbf{R}) = \frac{2a_0}{R} \text{erf} \left[\frac{R}{\sqrt{2}\sigma} \right] \text{Ry} + \epsilon_{eb} \quad (65)$$

with ϵ_{bb} given by (62). We can then see immediately that by simply taking the sum of kinetic and renormalized potential energies at the spherical cell level [see Eq. (66) below] we already reproduce the correct result (60). Notice that $U(0,0,\mathbf{R})$ is now negative, a crucial fact for the stability of the spin-singlet paired lattice.

The above operations at the cell level are indeed completely equivalent to the subtraction of the $\mathbf{q}=0$ term in the potential energy, as can be seen from the exact result for the extensive energy in the extremely low-density limit. This, for N electrons, turns out to be simply

$$E = NT(0) + \frac{1}{2} \sum_{i \neq j} U(0,0,\mathbf{R}_{ij}), \quad (66)$$

and the $\mathbf{q} \neq 0$ restriction in the definition of $U(0,0,\mathbf{R})$ [see (68) below] will give the correct Madelung energy. Now, it is a well-known fact that the absent $\mathbf{q}=0$ term of the sum, had it been included, would actually cancel the (electron-background) + (background-background) interaction energy. We therefore conclude that if we wish to use a $U(0,0,\mathbf{R})$, but in a cell approximation that gives the correct Madelung energy within the same approximation, then we must use

$$\epsilon = 2T(0) + U(0,0,\mathbf{R}) + \epsilon_{bb} \quad (67)$$

for the energy per pair, but with $U(0,0,\mathbf{R})$ as given by (65).

An alternative way of seeing that the renormalization (65) is the physically appropriate one is in fact to show that it is actually equivalent to adding the harmonic background well to the *total* interaction experienced by the two electrons in each spherical cell. Indeed, by definition

$$U(0,0,\mathbf{R}) = \sum_{\mathbf{q} \neq 0} \frac{4\pi e^2}{Vq^2} e^{i\mathbf{q} \cdot \mathbf{R}} \int d^3k d^3k' f(\mathbf{k}' + \mathbf{q}) \\ \times f(\mathbf{k} - \mathbf{q}) f(\mathbf{k}') f(\mathbf{k}). \quad (68)$$

If, for a moment, we keep the *unconstrained* sum $\sum_{\mathbf{q}}$, then, as we have shown earlier [and also in Appendix A, Eq. (A52)] with Gaussian choices for f , we obtain the pure electron-electron repulsion $(2a_0/R) \text{erf}(R/\sqrt{2}\sigma)$. But transformation of this sum back to real space gives

$$\int d^3r d^3r' \frac{e^2}{|\mathbf{R} - \mathbf{r} + \mathbf{r}'|} f(\mathbf{r})^2 f(\mathbf{r}')^2,$$

which with change of variables to $\mathbf{r}_1 = \mathbf{r} - \mathbf{R}/2$ and $\mathbf{r}_2 = \mathbf{r}' + \mathbf{R}/2$ gives

$$\int d^3r_1 d^3r_2 f(\mathbf{r}_1 - \tilde{\mathbf{R}}_1)^2 \frac{e^2}{|\mathbf{r}_1 - \mathbf{r}_2|} f(\mathbf{r}_2 - \tilde{\mathbf{R}}_2)^2,$$

with $\tilde{\mathbf{R}}_1 \equiv -\mathbf{R}/2$ and $\tilde{\mathbf{R}}_2 \equiv \mathbf{R}/2$. This is merely the direct Coulomb repulsion element if \mathbf{r}_1 and \mathbf{r}_2 are integrated over *all* space. The point, however, is that we are required to consider the *lattice* environment, as well as the presence of the background. Each pair of electrons only samples the space in one cell; but each electron also feels an attraction from the background. Therefore, in a spherical cell approximation, the integrations are constrained to a spherical cell and we must also replace the pure Coulomb repulsion by the *total* interaction

$$\frac{e^2}{|\mathbf{R} - \mathbf{r} + \mathbf{r}'|} - [|eV_b(\mathbf{r})| + |eV_b(\mathbf{r}')|].$$

The background potential V_b is given by (59). We therefore obtain the renormalized Coulomb element as

$$U(0,0,\mathbf{R}) = \int_{\text{sphere}} d^3r d^3r' \left[\frac{e^2}{|\mathbf{R} - \mathbf{r} + \mathbf{r}'|} \right. \\ \left. - [|eV_b(\mathbf{r})| + |eV_b(\mathbf{r}')|] \right] \\ \times f(\mathbf{r})^2 f(\mathbf{r}')^2, \quad (69)$$

which after the integrations gives exactly the same result (65).

Accordingly the full result involving pure intrapair exchange is

$$\epsilon_{\text{intra}} = \frac{2T(0) + U(0,0,\mathbf{R}) + 2S(\mathbf{R})T(\mathbf{R}) + U(\mathbf{R}, -\mathbf{R}, \mathbf{R})}{1 + S(\mathbf{R})^2} \\ + \epsilon_{bb} \quad (70)$$

for the energy per pair, with $U(0,0,\mathbf{R})$ given by (65). This is exactly the same result [Eq. (A57)] that we obtain in Appendix A with a standard (but simpler) Heitler-London procedure in first quantization, as would actually be expected for a single pair. This result, as discussed in Appendix A, actually generalizes a previous result¹³ obtained for the orientationally averaged $\langle \text{Pa3} \rangle$ structure, to the dynamic case ($\sigma \neq 0$). In the extremely low-density limit the exchange effect vanishes and the asymptotically limiting value for the energy per particle is

$$-\frac{(\frac{21}{10})/2^{1/3}}{r_s} + \frac{3}{r_s^{3/2}} \text{Ry}. \quad (71)$$

Having secured the lowest-order result in the Heitler-London description, we can now directly proceed to the next-order correction, which, as discussed earlier, essentially involves the exact solution of a $2(n+1)$ -electron problem, namely a close-packed cluster consisting of a central pair and all n neighboring pairs. Our second quantized description will now *automatically* give the *combined* intrapair and interpair exchange effect on the ground-state energy, which is an advantage relative to the simpler first quantization procedure of Appendix A.

For clarity let us first consider the exact solution for two pairs (i.e., consider only one neighboring pair $n=1$). There are four electrons in two pairs [see Fig. 4(a)], each pair being a spin-singlet Heitler-London combination of two single-particle states f , centered at \mathbf{R}_1 and \mathbf{R}_2 for the first pair and at \mathbf{R}_3 and \mathbf{R}_4 for the second pair. The center of mass, or equivalently the center of the cell, of the first pair is $(\mathbf{R}_1 + \mathbf{R}_2)/2$ and of the second pair is $(\mathbf{R}_3 + \mathbf{R}_4)/2$, and these represent "lattice sites." Although the results will be general and will only depend on the four vectors \mathbf{R}_i and on the form of f , at the end we will consider pairs of identical sizes represented by a common internal order parameter \mathbf{R} , namely $|\mathbf{R}_1 - \mathbf{R}_2| = |\mathbf{R}_3 - \mathbf{R}_4| \equiv R$. The orientation of the two pair axes will for the moment be left general (but fixed).

The result we obtain for $N=4$ is lengthy but straightforward to obtain and to evaluate, namely

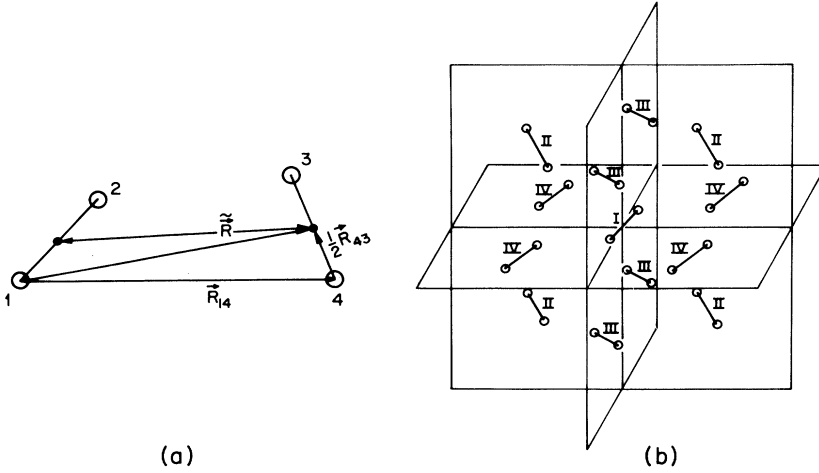


FIG. 4. (a) Four electrons in two pairs; (b) a cluster of 26 electrons for the Pa3 structure [one central pair (of direction I) and the set of the 12 nearest-neighbor pairs (of three distinct directions II, III, and IV)]. Directions I, II, III, and IV denote the orientations along the four possible choices of body diagonal for the conventional cube of Fig. 1(b).

$$\begin{aligned}
 \langle \Psi | H | \Psi \rangle = N & \left[NT(0) + \frac{1}{2} \sum_{i \neq j}^{N, N} U(0, 0, \mathbf{R}_{ij}) + 2[T(12)S(12) + T(34)S(34)] + [U(21, 12, 21) + U(43, 34, 43)] \right. \\
 & + \{ [T(33) + T(44)]S(12)^2 + [T(11) + T(22)]S(34)^2 \} + [S(12)^2 U(0, 0, 34) + S(34)^2 U(0, 0, 12)] \\
 & + [U(0, 43, 14)S(34) + U(0, 34, 13)S(34) + U(0, 43, 24)S(34) + U(0, 34, 23)S(34) \\
 & \left. + U(21, 0, 23)S(12) + U(21, 0, 24)S(12) + U(12, 0, 13)S(12) + U(12, 0, 14)S(12)] + \Delta E + O(S^4) \right] \quad (72)
 \end{aligned}$$

with

$$\begin{aligned}
 \Delta E = & -[T(13)S(13) + T(24)S(24) + T(23)S(23) + T(14)S(14)] \\
 & - \frac{1}{2}[U(13, 31, 13) + U(24, 42, 24) + U(32, 23, 32) + U(41, 14, 41)] - T(0)[S(13)^2 + S(24)^2 + S(23)^2 + S(14)^2] \\
 & - \frac{1}{2}[U(0, 0, 13)S(24)^2 + U(0, 0, 24)S(13)^2 + U(0, 0, 23)S(14)^2 + U(0, 0, 14)S(23)^2] \\
 & - \frac{1}{2}[U(13, 0, 12)S(13) + U(13, 0, 14)S(13) + U(24, 0, 23)S(24) + U(31, 0, 34)S(13) \\
 & + U(0, 24, 12)S(24) + U(0, 42, 14)S(24) + U(0, 31, 23)S(13) + U(0, 42, 34)S(24) \\
 & + U(32, 0, 12)S(23) + U(32, 0, 42)S(23) + U(41, 0, 31)S(14) + U(23, 0, 43)S(23) \\
 & + U(0, 41, 12)S(14) + U(0, 14, 42)S(14) + U(0, 23, 31)S(23) + U(0, 14, 43)S(14)] \quad (73)
 \end{aligned}$$

and

$$\begin{aligned}
 \langle \Psi | \Psi \rangle = N & \{ 1 + 2S(\mathbf{R})^2 \\
 & - \frac{1}{2}[S(13)^2 + S(24)^2 + S(23)^2 + S(14)^2] \\
 & + O(S^4) \} \quad (74)
 \end{aligned}$$

This is to be compared with an ‘‘antiferromagnetic arrangement’’ of four electrons with definite spins ($1\uparrow, 2\downarrow, 3\uparrow, 4\downarrow$) in the Wigner crystal example given in (13) in Sec. II.

The first two terms in (72) [and also in (13)] lead to the result (66) without exchange found earlier; together with the next two terms in (72) they lead to the single-pair result obtained in (48). The second, third, and fourth rows are the dominant interpair contributions as will be shown below. The remaining terms, denoted by ΔE , are all exponentially smaller since they are of order $S(\bar{R})^2$ with \bar{R}

interpair distances (i.e., distances between electrons belonging to distinct pairs), all higher than (and in general twice as large as) the intrapair distance R . Notice also that these terms [Eq. (73)] have a structure which is similar to the exchange contribution (15) in the Wigner crystal, denoted by ΔE_{ex} , and for the special choice of orientational states (to be considered below) they are in fact exactly equal. This is attributable to the fact that for such states all interpair distances appearing in (73) or in (15) are equal to each other and also equal to the distance between the two cell centers [see (79) and Fig. 4(a)].

We are then allowed to ignore the common and much smaller terms denoted by ΔE in (72), and retain only the dominant terms which, as we will see, happen to have an ‘‘intrapair appearance.’’¹ Indeed the first two terms in (72) can be written

$$NT(0) + \frac{N}{2}U(0,0,\mathbf{R}) \quad (75)$$

since this, with the renormalized element $U(0,0,\mathbf{R})$, has been proven in (67) to give the correct Madelung energy. The next two terms in (72) can be written

$$4T(\mathbf{R})S(\mathbf{R}) + 2U(\mathbf{R}, -\mathbf{R}, \mathbf{R}) \quad (76)$$

as in the single pair case (48). The second, third, and fourth, rows in (72) are an interpair effect since they *always* couple overlaps within one pair with elements T and U having arguments at the *other* pair. However, all these terms can at the end be written as proportional to $S(R)^2$, with R the intrapair distance. This is important since they can then be viewed as an *effective* intrapair correction.¹ As an example, the second row of (72) is just

$$4T(0)S(\mathbf{R})^2 + 2S(\mathbf{R})^2U(0,0,\mathbf{R}) \quad (77)$$

For the third row let us first consider the term $U(0,43,14)S(34)$: with the use of (54) for Gaussian choice of single-particle states, this term finally reads

$$S(\mathbf{R})^2 \frac{2a_0}{\tilde{R}} \operatorname{erf} \left[\frac{\tilde{R}}{\sqrt{2}\sigma} \right] \quad \text{Ry} \quad (78)$$

where $\tilde{R} \equiv |\mathbf{R}_{14} + \mathbf{R}_{43}/2|$ is the distance between "electron 1" and the *center* of the cell containing the pair 34 [see Fig. 4(a)]. Again it is proportional to $S(R)^2$. Similarly, it is straightforward to see that all eight terms in the third and fourth rows of (72) also turn out to have the same form (78), with \tilde{R} always being the distance of each electron from the center of the cell of the neighboring pair. In the case of an orientationally averaged structure (i.e., $\langle \text{Pa3} \rangle$), all these \tilde{R} 's turn out to be equal to each other and actually equal to the distance between the two

cell centers, hence we must take

$$\tilde{R} = 2r_{\text{ws}} = 2 \times 2^{1/3} r_s a_0 \quad (79)$$

for spherical cells. These interpair terms, all being of $O[S(\mathbf{R})^2]$, are comparable to the pure intrapair terms (76), and are in fact the dominant terms compared to ΔE .

The terms just discussed are indeed corrections to the lowest-order (single-pair) result. In this case of two localized pairs the recursive method, introduced earlier for the delocalized case, will therefore give just the pure intrapair result (48) proportional to $|C|^2$ (as shown in Sec. III B 1), plus the additional interpair terms of (72) but now multiplied by $|C|^4$. This arises in exactly the way that the expansion of the delocalized result in powers of λ^2 was discussed in Sec. III A. The constant $|C|^2$ is determined self-consistently to lowest order in (37), and this value gives a $|C|^4 \sim [1 + S(\mathbf{R})^2]^{-2}$, which is consistent with the result (74) for the normalization constant, after the omission of the negligibly small terms $S(\tilde{R})^2$, with \tilde{R} interpair distances, discussed above. This follows from the fact that $[1 + 2S(\mathbf{R})^2] \simeq [1 + S(\mathbf{R})^2]^2$, so long as we only keep terms to $O[S(\mathbf{R})^4]$.

The result therefore is that, if we had but a single pair ($n=1$) as a neighbor to our "central" pair, the low-density series expansion would give for the energy *per electron*

$$\frac{E}{N} = \frac{T(0) + \frac{1}{2}U(0,0,\mathbf{R}) + S(\mathbf{R})T(\mathbf{R}) + \frac{1}{2}U(\mathbf{R}, -\mathbf{R}, \mathbf{R})}{1 + S(\mathbf{R})^2} + \frac{1}{2}\epsilon_{bb} + \Delta E_{\text{inter}}^{(n)} \quad (80)$$

where, as we found above

$$\Delta E_{\text{inter}}^{(n=1)} = \frac{S(\mathbf{R})^2 [T(0) + \frac{1}{2}U(0,0,\mathbf{R})] + 2S(\mathbf{R})^2 \frac{2a_0}{\tilde{R}} \operatorname{erf} \left[\frac{\tilde{R}}{\sqrt{2}\sigma} \right]}{[1 + S(\mathbf{R})^2]^2} \quad (81)$$

for the interpair correction. However, in the actual three-dimensional lattice, we *must* use a close-packed cluster in order to study the interpair effect and in particular to determine how it "propagates" through the neighbors to the entire crystal. The chosen cluster consists of a central pair and $n=12$ neighboring pairs (26 electrons in total). Applying exactly the same analysis to such a case we obtain

$$\Delta E_{\text{inter}}^{(n)} = \frac{nS(\mathbf{R})^2 [T(0) + \frac{1}{2}U(0,0,\mathbf{R})] + 2nS(\mathbf{R})^2 \frac{2a_0}{\tilde{R}} \operatorname{erf} \left[\frac{\tilde{R}}{\sqrt{2}\sigma} \right]}{[1 + S(\mathbf{R})^2]^{n+1}} \quad (82)$$

since now the correction is of $O(|C|^2)^{n+1}$, as can be seen from application of the recursion method to this $2(n+1)$ -electron problem. In the above we set $n=12$, \tilde{R} is given by (79), and for reasons of self-consistency it is important to keep the renormalized value (65) for *every* cell, central or neighboring. This is because all cells are equivalent, in the sense that any cell initially chosen as a neighboring one can always be considered as a central one in a new calculation. This self-consistency is vital in describing the propagation of these exchange correlations

through the entire three-dimensional crystal and it is a variant of the Bethe approximation in the theory of critical phenomena. Note again that the "no-exchange" Madelung energy is indeed given by $\frac{1}{2}U(0,0,\mathbf{R}) + \frac{1}{2}\epsilon_{bb}$ per electron, in agreement with (67).

IV. RESULTS AND DISCUSSION

Our final result for the energy per electron is (80), with $\Delta E_{\text{inter}}^{(n)}$ given by (82) for $n=12$. For every fixed r_s and R

we minimize the above with respect to σ and then by using the optimum values of σ we minimize with respect to R . A typical minimization procedure is shown for $r_s = 100$ in Fig. 2, where we see that for this density the optimal values for the pair size and half width are $R_0 \approx 110a_0$ and $\sigma_0 \approx 43a_0$, respectively. For these values we observe that the energy of the $\langle Pa3 \rangle$ structure is *lower* than the conventional bcc structure. These results reproduce those published recently¹ for the paired crystal through an *effective* single-cell method which described the interpair effect in an orientationally averaged crystal through anharmonic potentials and variational wave functions in an effective cell.

The final results for the energetics of the paired crystal for various densities are shown in Fig. 3, where they are compared with Monte Carlo results¹⁴ for the conventional monatomic (Wigner) crystal. We conclude that the paired crystal is energetically favored over the monatomic crystal for densities not too low, namely for $r_s \lesssim 200$. For higher densities ($r_s < 100$) the paired states seem to be even more favored, as already discussed, but in that range we begin to develop charge leakage [violation of assumption (A22) in the spherical cell method] so that our method allows us to focus on the range $r_s \gtrsim 100$ only.

At this point it is worth commenting that the same general analysis as given above can be straightforwardly applied to short-ranged (i.e., Lennard-Jones or similar) interactions between fermions (as in He³). This is done in Appendix C and it gives a practically vanishing contribution for the exchange effects studied above. The analysis confirms that most of the energy gain is at long range. The conclusions are therefore that exchange effects are important in structured low-density systems with Coulomb interactions and especially so when coherence effects are present; furthermore it is possible to address them (in the ground state) through a second quantized variational method. As a result, paired structures, both true crystalline and orientationally averaged (including orientational glasses), seem highly likely in three dimensions and they can be viewed as exchange-driven three-dimensional Peierls dimerizations. A by-product of such an analysis is the generalization of the concept of a super-solid, from condensed localized neutral bosons (He⁴) to condensed paired localized charged fermions, with an interesting coexistence of diagonal and off-diagonal long-range order. If this pairing condensation persists beyond melting (where we have the case of diffusive pairs and superconductivity, as discussed in the text) then we can expect a form of superconductivity due to a novel exchange mechanism. The two-dimensional generalization of this work is therefore interesting for reasons associated with the recently found unconventional superconductors and their universal behavior.¹⁵ Extensions of the present work to $r_s < 100$ requires a different method, such as, for example, simulation or analytical techniques¹⁶ capable of searching for exchange and correlation-induced pairing at higher densities in systems with large numbers of electrons. It should also be noted that paired structures with $S = 0$ spin pairing of the type considered above were also reported recently¹⁷ for two-dimensional systems in a magnetic field in the extreme quantum limit, so that the

theoretical inclusion of a magnetic field in the above approach should also be an interesting problem.

Finally we return to the paper of Abarenkov.³ The principal assumption made there in the final computation relates to the sign of some index-dependent exchange-correlation energy matrix elements which are taken as independent of pair indices and all positive; what we find is that the types of indices are important. For indices belonging to the same pair those elements *are* positive due to the stability of the singlet paired state in the background well; but for indices belonging to distinct pairs those elements are negative (as would actually be expected if the separation of the two indices approached infinity). Although therefore the basic description in Ref. 3 is similar to ours,¹ the philosophy adopted in that paper is different: the basic calculation there consists of a central *site* surrounded by the first neighboring *sites*. In our case the basic calculation consists of a higher cluster, namely a central *pair* surrounded by the first neighboring *pairs*, all described in a self-consistent fashion. This difference is crucial for orientationally averaged structures, since for such structures the effect of next-neighboring sites is obviously important [see Fig. 4(a)]. Also our description, in contrast to the one in Ref. 3, basically describes the coherence properties of a paired super-solid, as explained in Sec. III.

ACKNOWLEDGMENTS

This work was supported by the National Science Foundation under Grant No. DMR-9017281. We also thank M. Taut and C. Umrigar for discussions on the comparisons between fully rotational and orientationally averaged paired states.

APPENDIX A: THE SPHERICAL CELL METHOD

1. Monatomic (Wigner) crystal

We begin with a brief review of the conventional Wigner crystal within the spherical cell model. As mentioned in the Introduction the unit cell of the monatomic crystal in this model is approximated by a sphere and the electron is considered localized around the center. For neutrality the sphere must have radius $r_s a_0$ so that the total charge (electron + background) within each sphere is zero. Since by Gauss's law the electric field outside each sphere is zero for sufficient localization, it is an excellent approximation that the Madelung energy for the crystal can be determined by a sum of contributions from distinct spheres, the error being insignificant for symmetric structures. In this model an electron only "feels" the background within its sphere under the proviso that the *total* potential on the surface of the sphere vanishes. The background therefore contributes a harmonic potential with the minimum at the center of the sphere (see below). It is then self-consistent to assume that the motion of the electron around the center is harmonic and we can estimate the energy per electron ϵ by two different methods: The first is standard¹⁸ and treats the electron as a point charge. The second uses a different picture for the electron, namely that of a smeared distribution of charge lo-

calized around the sphere center. We will see that the second method is better suited for our purpose of generalizing the model to the paired crystal, because (a) it provides a variational method with respect to the width of the distribution and (b) it can treat intrapair exchange in an "obvious" way namely through a Heitler-London combination of single-particle distributions.

a. Point-charge approach

In this standard picture the electron, viewed as a point charge, is kept strictly localized around the center because of the attraction from the background. The energy ϵ_{eb} of this interaction can be determined either by the integral of the uniform background charge density multiplied by the potential of the point charge, namely (with $\rho = 3/4\pi r_s^3 a_0^3$ and $r_{ws} = r_s a_0$)

$$\epsilon_{eb} = \rho e \int_0^{r_{ws}} 4\pi r^2 dr \left[-\frac{e}{r} \right] = -\frac{3}{r_s} \text{Ry} \quad (\text{A1})$$

or, equivalently, by the integral of the point-charge density multiplied by the potential of the background, namely

$$\epsilon_{eb} = \int d^3r [-e\delta(\mathbf{r})] V_b(\mathbf{r}) = -eV_b(0). \quad (\text{A2})$$

Now $V_b(r)$ can be determined either by Gauss's law or by direct integration, with the constraint that the *total* potential vanishes on the surface of the sphere, namely $V_b(r_{ws}) - e/r_{ws} = 0$. An elementary calculation yields

$$V_b(r) = -\frac{e}{2r_s^3 a_0^3} r^2 + \frac{3}{2} \frac{e}{a_0 r_s} \quad (\text{A3})$$

giving therefore

$$\epsilon_{eb} = -\frac{3}{r_s} \text{Ry}, \quad (\text{A4})$$

in agreement with (A1). The Madelung energy is then given by

$$\epsilon_M = \epsilon_{eb} + \epsilon_{bb} \quad (\text{A5})$$

where the interaction of the background with itself is

$$\epsilon_{bb} = \frac{1}{2} \rho e \int_0^{r_{ws}} 4\pi r^2 dr V_b(r) \quad (\text{A6})$$

and with the use of (A3) yields

$$\epsilon_{bb} = \frac{6}{5r_s} \text{Ry}. \quad (\text{A7})$$

Finally the total energy per electron in this point-charge picture is

$$\epsilon = \epsilon_M + \epsilon_k + \epsilon_p \quad (\text{A8})$$

with $\epsilon_k = \epsilon_p = \frac{3}{4} \hbar\omega$ for the kinetic and potential energies of the oscillator. But from (A3) and the fact that the potential energy of the electron is $-eV_b(r)$ we obtain

$$\omega^2 = \frac{4\pi\rho e^2}{3m} = \frac{e^2}{mr_s^3 a_0^3}, \quad (\text{A9})$$

or equivalently

$$\hbar\omega = \frac{2}{r_s^{3/2}} \text{Ry}. \quad (\text{A10})$$

Hence (A8) finally yields

$$\epsilon = -\frac{9}{5r_s} + \frac{3}{r_s^{3/2}} \text{Ry}, \quad (\text{A11})$$

which is the well-known result in this model. However, the method is not easily generalizable to the paired case; so we next consider an alternative.

b. Distributed-charge approach

In this picture we recognize as an immediate consequence of zero-point motion the distributed nature of the electron as a charge density $-e\rho(r)$ localized around the center. The Madelung energy is again given by (A5) with ϵ_{bb} given by (A6); the background potential is now

$$V_b(r) = -\frac{e}{2r_s^3 a_0^3} r^2 + C \quad (\text{A12})$$

with the constant C determined by

$$V_b(r_{ws}) + V(r_{ws}) = 0 \quad (\text{A13})$$

where in this case $V(r)$ is the potential of the smeared charge distribution, which is generally different from that of a point charge. Once again this can be found either from Gauss's law or from direct integration and the result for an isotropic $\rho(r)$ is given by

$$V(r) = -e \int \frac{dr}{r^2} \int_0^r 4\pi r'^2 dr' \rho(r') + \tilde{C}, \quad (\text{A14})$$

where the constant \tilde{C} is chosen in such a way that $\lim_{r \rightarrow \infty} V(r) = 0$. However, we will assume normalization, namely

$$\int_{\text{sphere}} d^3r \rho(\mathbf{r}) \simeq 1, \quad (\text{A15})$$

which is valid whenever the width of the charge distribution is small compared to the radius of the sphere $r_s a_0$ (see below). Under these conditions $V(r_{ws}) \simeq -e/r_{ws}$, i.e., V has the form of a point charge when viewed from the surface. Hence V_b is still given by (A3) and ϵ_{bb} is still given by (A7). Including the proviso (A15) at every step, the major differences then with the standard point-charge approach are the following.

(i) *In the calculation of ϵ_{eb} .* This is again determined either by the integral of the product of the uniform background charge density with the potential $V(\mathbf{r})$ originating with the smeared electronic charge

$$\epsilon_{eb} = \int_{\text{sphere}} d^3r (e\rho) V(\mathbf{r}) \quad (\text{A16})$$

or alternatively by the integral of the product of the smeared charge density with the potential of the background

$$\epsilon_{eb} = \int_{\text{sphere}} d^3r [-e\rho(\mathbf{r})] V_b(\mathbf{r}). \quad (\text{A17})$$

These expressions are further used in *c*, for a particular choice of $\rho(\mathbf{r})$.

(ii) *In the calculation of the total energy per electron ϵ .*

In sharp contrast with the point-charge approach, the above calculation of ϵ_{eb} for the smeared charge has *already included* what was the potential energy ϵ_p of the motion of the point charge in the method in Sec. A 1 a. [For example, we will see that in the oscillator case, the positive potential energy ϵ_p appearing in Sec. A 1 a will be equal to the increase of the Madelung energy due to the smearing of the charge; combine below Eqs. (A27) and (A30).] As a result the total energy per electron is now given by

$$\epsilon = \epsilon_{bb} + \epsilon_{eb} + \epsilon_k \quad (\text{A18})$$

rather than (A8). The kinetic energy ϵ_k of the electron can be found from the wave function describing its motion around the center (Sec. A 1 c below).

This picture provides us with a variational method since we can vary the final result for ϵ with respect to the width of the charge distribution and subsequently determine the energy (A18) at the minimum. Below we use this method for the harmonic monatomic crystal.

c. Application of method b to a Gaussian distribution

Consider the electron in each Wigner-Seitz sphere to be distributed around the center through a Gaussian wave function, namely

$$\Psi(r) = \left[\frac{m\omega}{\pi\hbar} \right]^{3/4} e^{-(m\omega/2\hbar)r^2} \quad (\text{A19})$$

corresponding to a single-particle density

$$\rho(r) = |\Psi(r)|^2 = \frac{1}{\pi^{3/2}\sigma^3} e^{-r^2/\sigma^2} \quad (\text{A20})$$

with the half width $\sigma = \sqrt{\hbar/m\omega}$. Because (A20) gives

$$\int_0^{r_{ws}} 4\pi r^2 dr \rho(r) = \text{erf} \left[\frac{r_{ws}}{\sigma} \right] - \frac{2}{\sqrt{\pi}} \frac{r_{ws}}{\sigma} e^{-r_{ws}^2/\sigma^2} \quad (\text{A21})$$

we must require

$$\sigma = \sigma(r_s) \ll r_{ws} \quad (\text{A22})$$

in order to satisfy neutrality (A15). For the densities of interest here, this turns out to be well satisfied. The potential $V(r)$ originating with this charge distribution is determined by (A14), the result being exactly

$$V(r) = -\frac{e}{r} \text{erf} \left[\frac{r}{\sigma} \right]. \quad (\text{A23})$$

Further, the background potential is determined by (A12) and (A13), the result being

$$V_b(r) = -\frac{e}{2r_s^3 a_0^3} r^2 + \frac{3}{2} \frac{e}{r_s a_0} - \left[1 - \text{erf} \left[\frac{r_{ws}}{\sigma} \right] \right] \frac{e}{a_0 r_s}, \quad (\text{A24})$$

which, with the assumption (A22), yields (A3) as discussed earlier. Correspondingly ϵ_{bb} as given by (A6) is

$$\epsilon_{bb} = \frac{\frac{1}{5} + \text{erf} \left[\frac{r_{ws}}{\sigma} \right]}{r_s} \text{Ry}, \quad (\text{A25})$$

which under (A22) yields (A7). For the interaction of the smeared charge distribution with the background, Eq. (A16) together with (A23) gives

$$\epsilon_{eb} = -\frac{3}{r_s} \left[1 - \frac{\sigma^2}{2r_{ws}^2} \right] \text{erf} \left[\frac{r_{ws}}{\sigma} \right] - \frac{3}{\sqrt{\pi}} \frac{\sigma}{r_{ws}} \frac{1}{r_s} \exp(-r_{ws}^2/\sigma^2) \text{Ry}, \quad (\text{A26})$$

which in the limit (A22) leads to

$$\epsilon_{eb} = -\frac{3}{r_s} + \frac{3}{2r_s^3} \frac{\sigma^2}{a_0^2} \text{Ry}. \quad (\text{A27})$$

[Alternatively, (A17) also gives in the limit (A22) the same result (A27), as expected.] Finally, ϵ_k is now determined with the use of (A19), the result being

$$\epsilon_k = \frac{3}{4} \hbar\omega = \frac{3}{2} \frac{a_0^2}{\sigma^2} \text{Ry}. \quad (\text{A28})$$

In the limit (A22) the total energy per electron ϵ is therefore given by

$$\epsilon = -\frac{9}{5r_s} + \frac{3}{2r_s^3} \frac{\sigma^2}{a_0^2} + \frac{3}{2} \frac{a_0^2}{\sigma^2} \text{Ry}, \quad (\text{A29})$$

which can be analytically minimized with respect to σ . The minimum occurs at

$$\sigma_0 = r_s^{3/4} a_0 \quad (\text{A30})$$

with a corresponding energy

$$\epsilon = -\frac{9}{5r_s} + \frac{3}{r_s^{3/2}} \text{Ry}, \quad (\text{A31})$$

which is identical to the point-charge result (A11). This should be physically expected because of the equivalence between the point-charge approach and the present approach as applied to a single Gaussian distribution. (It was already mentioned, for example, that the potential energy of the harmonic motion of the point charge in the former approach is accounted for in the present approach as an electrostatic energy of the interaction of the smeared charge distribution with the background.)

As mentioned earlier, the other benefit of this approach beyond its variational character is that it can handle intrapair exchange within a paired state through a Heitler-London approach, a case where the point-charged approach A 1 a is not obviously generalizable. The above method is essentially equivalently to the "self-consistent phonon" method, but applied to an Einstein oscillator.

2. The paired crystal

We follow a similar approach for a crystal now composed of $N/2$ electron pairs and again use the Wigner-

Seitz model. In particular we consider in each sphere of volume $V/(N/2)$ a Heitler-London pair of electrons in a spin-singlet configuration. In this simple way, we essentially account for intrapair exchange through a first quantization approach which is complementary to (and will give the same results for a single pair with) the complete second quantized approach followed in the main text. Again we will make a self-consistent argument and assume orientationally uncorrelated states, so that at the end an orientational average can be taken. In such a state no additional higher multipole contributions arise (on the average) from any pair, and because of this the assumed orientationally averaged pair state can indeed be self-consistently sustained. The total energy is then again a sum of contributions from distinct spheres; the total energy per pair can then be determined again by consideration of a single sphere (but now of radius $r_{\text{WS}}=2^{1/3}r_s a_0$). Under these assumptions the total energy *per particle* is

$$\epsilon = \frac{1}{2}(\epsilon_{bb} + \epsilon_{eb} + \epsilon_{\text{HL}}) \quad (\text{A32})$$

where ϵ_{HL} is the energy of an assumed two-particle Heitler-London variational state in each pair. This includes the total kinetic energy for the pair and the potential energy due to the electron-electron repulsion (the potential energy due to the interaction with the background is again included in the ϵ_{eb} similarly as in A 1 b). As noted above it is useful to use Gaussian trial states, namely

$$\Psi(\mathbf{r}, \mathbf{r}') = \frac{1}{\sqrt{2(1+S^2)}} [\psi_1(\mathbf{r})\psi_2(\mathbf{r}') + \psi_1(\mathbf{r}')\psi_2(\mathbf{r})] \quad (\text{A33})$$

with

$$\psi_i(\mathbf{r}) = \frac{1}{\pi^{3/4}\sigma^{3/2}} e^{-(1/2)[(\mathbf{r}-\mathbf{R}_i)^2/\sigma^2]}, \quad i=1,2. \quad (\text{A34})$$

These are symmetrically placed around the center of the cell, they are separated by $\mathbf{R}(\equiv \mathbf{R}_2 - \mathbf{R}_1)$ and they have overlap

$$S(\mathbf{R}) = \int d^3r \psi_1^*(\mathbf{r})\psi_2(\mathbf{r}) = e^{-R^2/4\sigma^2}. \quad (\text{A35})$$

The single-particle density corresponding to this state is determined by

$$\rho_{\text{HL}}(\mathbf{r}) = \left\langle \sum_{i=1}^2 \delta(\mathbf{r} - \mathbf{r}_i) \right\rangle_{\text{HL}} = 2 \int d^3r' |\Psi(\mathbf{r}, \mathbf{r}')|^2 \quad (\text{A36})$$

and is of the form

$$\rho_{\text{HL}}(\mathbf{r}) = \frac{1}{1+S^2} \left[\psi_1^2(\mathbf{r}) + \psi_2^2(\mathbf{r}) + 2S^2 \frac{1}{\pi^{3/2}\sigma^3} e^{-r^2/\sigma^2} \right]. \quad (\text{A37})$$

Note the effect of exchange: it adds a third peak around the center (what might be called "bond charge," a term used, for example, in the physics of semiconductors), although the total density is renormalized by $1/(1+S^2)$ to comply with normalization, namely

$$\int_{\text{sphere}} d^3r \rho_{\text{HL}}(\mathbf{r}) = 2. \quad (\text{A38})$$

[The case of no exchange is formally described by the

statement $S=0$, which would be equivalent to a single product of two Gaussian functions in (A33) and correspondingly a simple sum of two single-electron densities in (A37).] Again we can determine ϵ_{bb} and ϵ_{eb} in closed form for arbitrary ratio σ/r_{WS} , by using (A6) and (A16) or (A17). However, it is still the limit $\sigma \ll r_{\text{WS}}$ that is of physical interest and this limit simplifies the results considerably. First, for ϵ_{bb} we obtain the expected result

$$\epsilon_{bb} = \frac{6}{5r_s} 2^{5/3} \text{Ry}. \quad (\text{A39})$$

Second, the term ϵ_{eb} can be written in terms of ρ_{HL} as

$$\epsilon_{eb} = \int d^3r [-e\rho_{\text{HL}}(\mathbf{r})]V_b(\mathbf{r}), \quad (\text{A40})$$

which is generalization of (A17), where now, however, $V_b(\mathbf{r})$ is given by

$$V_b(\mathbf{r}) = -\frac{e}{2r_s^3 a_0^3} r^2 + \frac{3e}{2^{1/3}r_s a_0} \quad (\text{A41})$$

instead of (A3). Alternatively ϵ_{eb} can be found by Eq. (A16) with $V(\mathbf{r})$ now being

$$V(\mathbf{r}) = -\frac{e}{1+S^2} \left[\frac{\text{erf}\left(\frac{|\mathbf{r}-\mathbf{R}_1|}{\sigma}\right)}{|\mathbf{r}-\mathbf{R}_1|} + \frac{\text{erf}\left(\frac{|\mathbf{r}-\mathbf{R}_2|}{\sigma}\right)}{|\mathbf{r}-\mathbf{R}_2|} + 2S^2 \frac{\text{erf}\left(\frac{r}{\sigma}\right)}{r} \right]. \quad (\text{A42})$$

In the limit (A22) both (A40) and (A16) yield

$$\epsilon_{eb} = -\frac{3}{r_s} 2^{5/3} + \frac{3}{r_s^3} \frac{\sigma^2}{a_0^2} + \frac{1}{2r_s^3} \frac{R^2}{a_0^2} \text{Ry}. \quad (\text{A43})$$

Finally we have to determine ϵ_{HL} . This is given by

$$\epsilon_{\text{HL}} = \left\langle \Psi \left| -\frac{\hbar^2}{2m} \nabla_1^2 - \frac{\hbar^2}{2m} \nabla_2^2 \right| \Psi \right\rangle + \left\langle \Psi \left| \frac{e^2}{|\mathbf{r}_1 - \mathbf{r}_2|} \right| \Psi \right\rangle \quad (\text{A44})$$

and can be determined by Fourier transformation of Ψ . Indeed, any of the averages in (A44) splits into a direct and an exchange term

$$\langle \Psi | h | \Psi \rangle = \frac{1}{1+S^2} (\langle AB | h | AB \rangle + \langle AB | h | BA \rangle). \quad (\text{A45})$$

For the direct kinetic-energy term we have

$$\begin{aligned} & \left\langle AB \left| -\frac{\hbar^2}{2m} \nabla_r^2 \right| AB \right\rangle \\ &= \int d^3r d^3r' \psi_1^*(\mathbf{r})\psi_2^*(\mathbf{r}') \left[-\frac{\hbar^2}{2m} \nabla_r^2 \right] \psi_1(\mathbf{r})\psi_2(\mathbf{r}'), \end{aligned} \quad (\text{A46})$$

which, after Fourier transformation

$$\psi_i(\mathbf{r}) = \int \frac{d^3q}{(2\pi)^3} \psi(\mathbf{q}) e^{i\mathbf{q}\cdot(\mathbf{r}-\mathbf{R}_i)} \quad (\text{A47})$$

with

$$\psi(\mathbf{q}) = (4\pi\sigma^2)^{3/4} e^{-\sigma^2 q^2/2}, \quad (\text{A48})$$

yields

$$\begin{aligned} \left\langle AB \left| -\frac{\hbar}{2m} \nabla_r^2 \right| AB \right\rangle &= \int \frac{d^3q}{(2\pi)^3} \frac{\hbar^2 q^2}{2m} \psi(\mathbf{q}) \psi(-\mathbf{q}) \\ &= \frac{3}{4} \hbar\omega = \frac{3}{2} \frac{a_0^2}{\sigma^2} \text{Ry}. \end{aligned} \quad (\text{A49})$$

For the exchange kinetic-energy term, the transformation (A47) leads to the result

$$\begin{aligned} \left\langle AB \left| -\frac{\hbar^2}{2m} \nabla_r^2 \right| BA \right\rangle &= \left[\int \frac{d^3q}{(2\pi)^3} \psi(\mathbf{q}) \psi(-\mathbf{q}) e^{-i\mathbf{q}\cdot(\mathbf{R}_1-\mathbf{R}_2)} \frac{\hbar^2 q^2}{2m} \right] \left[\int \frac{d^3q}{(2\pi)^3} \psi(\mathbf{q}) \psi(-\mathbf{q}) e^{i\mathbf{q}\cdot(\mathbf{R}_1-\mathbf{R}_2)} \right] \\ &= \left[\frac{3}{4} \hbar\omega S \left[1 - \frac{R^2}{6\sigma^2} \right] \right] (S) = \frac{3}{4} \hbar\omega S^2 \left[1 - \frac{R^2}{6\sigma^2} \right]. \end{aligned} \quad (\text{A50})$$

The two-particle kinetic energy is therefore found to be

$$\epsilon_{\text{kin}} = 3 \frac{a_0^2}{\sigma^2} \left[1 - \frac{S^2}{1+S^2} \frac{R^2}{6\sigma^2} \right] \text{Ry}. \quad (\text{A51})$$

Note that the effect of exchange is a reduction in kinetic energy because of the tunneling between the two centers. The above result is equal to (38) for $N=2$, which was derived in the main text through a second quantization procedure, and also equal to $[2T(0)+2S(R)T(R)]/[1+S(R)^2]$ with $T(0)$ given by (55) and $T(R)$ by (56), a result expected from the kinetic-energy part of the result (48). For the electron-electron repulsion, the direct term becomes

$$\begin{aligned} \left\langle AB \left| \frac{e^2}{|\mathbf{r}-\mathbf{r}'|} \right| AB \right\rangle &= \int \frac{d^3q}{(2\pi)^3} \int \frac{d^3q'}{(2\pi)^3} \psi(\mathbf{q}) \psi(\mathbf{q}') \int \frac{d^3\bar{q}}{(2\pi)^3} \psi(-\mathbf{q}-\bar{\mathbf{q}}) \psi(\bar{\mathbf{q}}-\mathbf{q}') \frac{4\pi e^2}{q^2} e^{i\mathbf{q}\cdot(\mathbf{R}_1-\mathbf{R}_2)} \\ &= \int \frac{d^3q}{(2\pi)^3} \frac{4\pi e^2}{q^2} e^{-\sigma^2 q^2/2} e^{i\mathbf{q}\cdot(\mathbf{R}_1-\mathbf{R}_2)} = \frac{e^2}{R} \text{erf} \left[\frac{R}{\sqrt{2}\sigma} \right] = \frac{2a_0}{R} \text{erf} \left[\frac{R}{\sqrt{2}\sigma} \right] \text{Ry}, \end{aligned} \quad (\text{A52})$$

which agrees with (57), while the exchange term is somewhat more involved but finally reads

$$\begin{aligned} \left\langle AB \left| \frac{e^2}{|\mathbf{r}-\mathbf{r}'|} \right| BA \right\rangle &= \int \frac{d^3q}{(2\pi)^3} \frac{4\pi e^2}{q^2} e^{-\sigma^2 q^2/2} e^{-i\mathbf{q}\cdot(\mathbf{R}_1-\mathbf{R}_2)} e^{-R^2/2\sigma^2} \\ &= S(R)^2 2\sqrt{2/\pi} \frac{a_0}{\sigma} \text{Ry}, \end{aligned} \quad (\text{A53})$$

which agrees with (58). The result is therefore

$$\epsilon_{\text{HL}} = \epsilon_{\text{kin}} + \epsilon_{\text{dir}} + \epsilon_{\text{ex}} \quad (\text{A54})$$

with ϵ_{kin} given by (A51) and with

$$\epsilon_{\text{dir}} = \frac{1}{1+S^2} \frac{2a_0}{R} \text{erf} \left[\frac{R}{\sqrt{2}\sigma} \right] \text{Ry} \quad (\text{A55})$$

and

$$\epsilon_{\text{ex}} = \frac{S^2}{1+S^2} 2\sqrt{2/\pi} \frac{a_0}{\sigma} \text{Ry}. \quad (\text{A56})$$

The result (A54) agrees with the second quantization result (48) for a single pair, as expected. Finally, Eq. (A32) takes the form

$$\epsilon = \frac{1}{2} (\epsilon_2 + \Delta\epsilon_{\text{ex}}) \quad (\text{A57})$$

where

$$\begin{aligned} \epsilon_2 &= 3 \frac{a_0^2}{\sigma^2} - \frac{9}{5r_s} 2^{5/3} + \frac{3}{r_s^3} \frac{\sigma^2}{a_0^2} \\ &+ \frac{1}{2r_s^3} \frac{R^2}{a_0^2} + \frac{2a_0}{R} \text{erf} \left[\frac{R}{\sqrt{2}\sigma} \right] \text{Ry} \end{aligned} \quad (\text{A58})$$

and is just the result we would have obtained had we ignored exchange [i.e., if the single-particle density (A37) were merely a sum of two displaced Gaussian functions]. The remainder

$$\begin{aligned} \Delta\epsilon_{\text{ex}} &= -\frac{S^2}{1+S^2} \left[\frac{2a_0}{R} \text{erf} \left[\frac{R}{\sqrt{2}\sigma} \right] + \frac{1}{2} \frac{a_0^4}{\sigma^4} \frac{R^2}{a_0^2} \right. \\ &\quad \left. - 2\sqrt{2/\pi} \frac{a_0}{\sigma} \right] \text{Ry} \end{aligned} \quad (\text{A59})$$

is then the correction due to the Heitler-London intrapair exchange and agrees with (70). Minimization of (A58) gives $\sigma_0 = r_s^{3/4} a_0$, $R_0 = r_{\text{ws}} = 2^{1/3} r_s a_0$, and an energy

$$\epsilon = -\frac{(\frac{21}{10})/2^{1/3}}{r_s} + \frac{3}{r_s^{3/2}} \text{Ry}, \quad (\text{A60})$$

which is *always* higher than its Bravais lattice analog (A31). The result (A58) is consistent with and in fact generalizes (to $\sigma \neq 0$) a previous result¹³ for the Madelung

energy of an isotropically averaged Pa3 structure ($\langle \text{Pa3} \rangle$), obtained with a lattice sum, namely

$$\epsilon = \frac{2^{2/3}}{r_s} \left[\alpha_{\text{fcc}} + \frac{1}{4z} + z^2 \right], \quad (\text{A61})$$

where $z = (R/2a)(16\pi/3)^{1/3}$ and a is the side of the underlying conventional cubic cell $a = 2r_s a_0 (4\pi/3)^{1/3}$, with the only replacement of the fcc Madelung constant $\alpha_{\text{fcc}} = -1.79175$ with $-\frac{9}{5}$, as should be expected from the use of the Wigner-Seitz sphere method. Inclusion of exchange (A59) alters these results only slightly, with the resulting energy very close to (A60) for low densities. We therefore conclude that at the level of Gaussian trial functions, pure intrapair exchange is not quite sufficient at low densities to promote pairing. [However, the lower the values of r_s , the larger the deviations from the above "classical" values and it turns out that pairing is actually favored at sufficiently high densities (around $r_s \sim 20$), although at such densities normalization (A15) within each sphere is no longer satisfied and we encounter charge "leakage" problems indicative that the liquid-homogeneous-phase is preferred.] Consideration therefore of the interpair effect is needed, and this is done through the second quantized approach as described in the main text (Sec. III). We find there that the interpair effect in a coherent paired supersolid can still be described at an *effective* cell level,¹ which in a range of densities leads to sufficient energy lowering to favor pairing.

APPENDIX B: ALGEBRAIC DETAILS

The evaluation of either $\langle W|H|W \rangle / \langle W|W \rangle$ [see (46)] or $\langle \Psi|H|\Psi \rangle / \langle \Psi|\Psi \rangle$ [see (45)] in the text is lengthy, but can be carried out in a straightforward way by repeated (and interconnected, whenever necessary) application of the following relations (B1)–(B3).

$$(1) \quad \{d_\sigma(\mathbf{R}), d_{\sigma'}^\dagger(\mathbf{R}')\} = \delta_{\sigma\sigma'} S(\mathbf{R}' - \mathbf{R}) \quad (\text{B1})$$

with the overlap S defined by (16). Relation (B1) results from (11) and the standard anticommutation relations

$$\begin{aligned} \delta E \equiv & \left[\sum_i \sum_{j \neq i} \delta_{s_i s_j} T(ij) S(ij) + \frac{1}{2} \sum_i \sum_{j \neq i} \delta_{s_i s_j} U(ij, ji, ij) + \frac{1}{2} \sum_i \sum_{j \neq i} \sum_{m \neq i, j} T(0) S(jm)^2 \delta_{s_m s_j} \right. \\ & + \frac{1}{2} \sum_i \sum_{j \neq i} \sum_{m \neq i, j} \delta_{s_m s_i} S(mi) U(im, 0, ij) + \frac{1}{2} \sum_i \sum_{j \neq i} \sum_{m \neq i, j} \delta_{s_m s_j} S(mj) U(0, jm, ij) \\ & \left. + \frac{1}{4} \sum_i \sum_{j \neq i} \sum_{m \neq i, j} \sum_{n \neq m, i, j} \delta_{s_m s_n} S(mn)^2 U(0, 0, ij) \right] \quad (\text{B5}) \end{aligned}$$

and

$$\langle W|W \rangle = 1 - \frac{1}{2} \sum_i \sum_{j \neq i} \delta_{s_i s_j} S(ij)^2 + O(S^4). \quad (\text{B6})$$

Similarly

$$\langle \Psi|H|\Psi \rangle = N \left\{ NT(0) + \frac{1}{2} \sum_i \sum_{j \neq i} U(0, 0, ij) - \frac{1}{2} \Delta E + \frac{1}{2} \tilde{\Delta} E + O(S^4) \right\} \quad (\text{B7})$$

$$\{c_{\mathbf{k}\sigma}, c_{\mathbf{k}'\sigma'}^\dagger\} = \delta_{\sigma\sigma'} \delta_{\mathbf{k}\mathbf{k}'}.$$

The strategy therefore is at every step to substitute $d_\sigma(\mathbf{R})d_{\sigma'}^\dagger(\mathbf{R}')$ by

$$\delta_{\sigma\sigma'} S(\mathbf{R}' - \mathbf{R}) - d_{\sigma'}^\dagger(\mathbf{R}') d_\sigma(\mathbf{R}).$$

(2)

$$H d_\sigma^\dagger(\mathbf{R}) = [H, d_\sigma^\dagger(\mathbf{R})] + d_\sigma^\dagger(\mathbf{R}) H \quad (\text{B2})$$

and

(3)

$$\begin{aligned} & [H, d_{\sigma_1}^\dagger(\mathbf{R}_1)] d_{\sigma_2}^\dagger(\mathbf{R}_2) \\ & = \{[H, d_{\sigma_1}^\dagger(\mathbf{R}_1)], d_{\sigma_2}^\dagger(\mathbf{R}_2)\} - d_{\sigma_2}^\dagger(\mathbf{R}_2) [H, d_{\sigma_1}^\dagger(\mathbf{R}_1)]. \end{aligned} \quad (\text{B3})$$

The repeated application of the above relations (until the operators d eventually encounter and annihilate the vacuum $|0\rangle$) leads to the final results for $\langle W|H|W \rangle / \langle W|W \rangle$ or $\langle \Psi|H|\Psi \rangle / \langle \Psi|\Psi \rangle$ (see below) which involve only three types of quantities: (i)

$$S(\mathbf{R}' - \mathbf{R})$$

defined by (16), as is obvious from the above; (ii)

$$\langle 0|d_{\sigma'}(\mathbf{R}') [H, d_\sigma^\dagger(\mathbf{R})] |0\rangle = \delta_{\sigma\sigma'} T(\mathbf{R} - \mathbf{R}'),$$

with T defined by (17); (iii)

$$\begin{aligned} & \langle 0|d_{\sigma_4}(\mathbf{R}_4) d_{\sigma_3}(\mathbf{R}_3) \{ [H, d_{\sigma_1}^\dagger(\mathbf{R}_1)], d_{\sigma_2}^\dagger(\mathbf{R}_2) \} |0\rangle \\ & = \delta_{\sigma_1 \sigma_3} \delta_{\sigma_2 \sigma_4} U(\mathbf{R}_1 - \mathbf{R}_3, \mathbf{R}_2 - \mathbf{R}_4, \mathbf{R}_1 - \mathbf{R}_2) \\ & \quad - \delta_{\sigma_1 \sigma_4} \delta_{\sigma_2 \sigma_3} U(\mathbf{R}_1 - \mathbf{R}_4, \mathbf{R}_2 - \mathbf{R}_3, \mathbf{R}_1 - \mathbf{R}_2), \end{aligned}$$

with U defined by (18).

The final results for arbitrary N are, to lowest order in the overlaps,

$$\langle W|H|W \rangle = NT(0) + \frac{1}{2} \sum_i \sum_{j \neq i} U(0, 0, ij) - \delta E + O(S^4) \quad (\text{B4})$$

with

with ΔE having the same form as δE but with any symbol $\delta_{s_k s_l}$ substituted by Δ_{kl} , and with $\tilde{\Delta} E$ also having the same form as δE but with any symbol $\delta_{s_k s_l}$ substituted by $\tilde{\Delta}_{kl}$, where the new symbols mean the following: Δ_{ij} , restriction of $\{i, j\}$ to all *interpair* possibilities (irrespective of spin); $\tilde{\Delta}_{ij}$, restriction of $\{i, j\}$ to all *intrapair* possibilities (which have only opposite spins). Finally, we also find

$$\langle \Psi | \Psi \rangle = N \left\{ 1 - \frac{1}{4} \sum_i \sum_{j \neq i} \Delta_{ij} S(ij)^2 + \frac{1}{2} \sum_i \sum_{j \neq i} \tilde{\Delta}_{ij} S(ij)^2 + O(S^4) \right\}. \quad (\text{B8})$$

APPENDIX C: APPLICATION TO SHORT-RANGED INTERACTIONS

We determine here the dominant interaction element $U(0,0,R)$ that corresponds to a system of localized He^3 atoms. In this case the interaction is short ranged and it can very accurately be described by a Lennard-Jones potential, namely

$$V_{\text{LJ}}(r) = 4\epsilon \left[\left(\frac{r_0}{r} \right)^{12} - \left(\frac{r_0}{r} \right)^6 \right]. \quad (\text{C1})$$

For He^3 the values of the parameters are $\epsilon/k_B = 10.2 \text{ K}$, or equivalently $\epsilon = 6.46 \times 10^{-5} \text{ Ry}$, and $r_0 = 2.56 \text{ \AA} = 4.84a_0$. It has been shown by Foiles and Ashcroft¹⁹

that this interaction can very accurately be described by a double Yukawa form, namely

$$V_{\text{DY}}(r) = \frac{A}{r} e^{-ar} - \frac{B}{r} e^{-br}, \quad (\text{C2})$$

which is a very convenient form for analysis. The potential (C2) matches (C1) extremely accurately if we take $A = Er_0 e^\alpha$, $B = Er_0 e^\beta$, $a = \alpha/r_0$, and $b = \beta/r_0$, with the definitions $E = 2.0199\epsilon$, $\alpha = 14.735$, and $\beta = 2.6793$.

Use of (C2) together with Gaussian wave functions with half width σ around the lattice sites gives for the direct interaction element

$$U(0,0,\mathbf{R}) = \int \frac{d^3q}{(2\pi)^3} V_{\text{DY}}(q) e^{-q^2\sigma^2/2 + iq \cdot \mathbf{R}} \quad (\text{C3})$$

with the Fourier transform $V_{\text{DY}}(q)$ of (C2) being

$$V_{\text{DY}}(q) = 4\pi \left[\frac{A}{q^2 + a^2} - \frac{B}{q^2 + b^2} \right]. \quad (\text{C4})$$

The integration in (C3) finally gives

$$U(0,0,R) = -\frac{1}{2R} \left\{ A e^{\sigma^2 a^2/2} \left[2 \sinh aR + e^{-aR} \operatorname{erf} \left[\frac{a\sigma}{\sqrt{2}} - \frac{R}{\sqrt{2}\sigma} \right] - e^{aR} \operatorname{erf} \left[\frac{a\sigma}{\sqrt{2}} + \frac{R}{\sqrt{2}\sigma} \right] \right] - B e^{\sigma^2 b^2/2} \left[2 \sinh bR + e^{-bR} \operatorname{erf} \left[\frac{b\sigma}{\sqrt{2}} - \frac{R}{\sqrt{2}\sigma} \right] - e^{bR} \operatorname{erf} \left[\frac{b\sigma}{\sqrt{2}} + \frac{R}{\sqrt{2}\sigma} \right] \right] \right\}. \quad (\text{C5})$$

This for values of $R > 10a_0$ is negligibly small, i.e., for $R = 110a_0$ and $\sigma = 43a_0$ we obtain $U(0,0,R) \simeq -10^{-5} \text{ Ry}$, which is negligible compared to the long-ranged analog (65), which for the same values of the parameters (corresponding to $r_s = 100$) has a value of -0.0657 Ry .

¹K. Mouloupoulos and N. W. Ashcroft, Phys. Rev. Lett. **69**, 2555 (1992); **70**, 2356 (1993).

²G. V. Shuster and A. I. Kozinskaya, Fiz. Tverd. Tela (Leningrad) **13**, 1240 (1971) [Sov. Phys. Solid State **13**, 1038 (1971)].

³I. V. Abarenkov, J. Phys. Condens. Matter **5**, 2341 (1993).

⁴E. P. Wigner, Phys. Rev. **46**, 1002 (1934); Trans. Faraday Soc. **34**, 678 (1938).

⁵N. W. Ashcroft, Phys. Rev. B **39**, 10 (1989); **39**, 552 (1989); Nature **340**, 345 (1989).

⁶J. Wilks, *The Properties of Liquid and Solid Helium* (Oxford University Press, Oxford, 1967), Chap. 22.

⁷G. V. Chester, Phys. Rev. A **2**, 256 (1970).

⁸W. J. Carr, Phys. Rev. **122**, 1437 (1961).

⁹W. Kohn (unpublished); see J. Bardeen and D. Pines, Phys. Rev. **99**, 1140 (1955), Appendix A.

¹⁰C. Domb and L. Salter, Philos. Mag. **43**, 1083 (1952).

¹¹L. G. J. van Dijk and G. Vertogen, J. Phys. Condens. Matter **3**, 7763 (1991).

¹²K. Mouloupoulos and N. W. Ashcroft, Phys. Rev. B **42**, 7855 (1990).

¹³D. M. Wood and N. W. Ashcroft, Phys. Rev. B **25**, 2532 (1982).

¹⁴D. M. Ceperley and B. J. Alder, Phys. Rev. Lett. **45**, 566 (1980).

¹⁵Y. J. Uemura, Physica C **185-189**, 733 (1991); Phys. Rev. Lett. **66**, 2665 (1991); Nature **352**, 605 (1991).

¹⁶Y. Takada, Phys. Rev. B **47**, 5202 (1993).

¹⁷R. Nicholas, Bull. Am. Phys. Soc. **38**, 249 (1993); G. M. Summers *et al.*, Phys. Rev. Lett. **70**, 2150 (1993).

¹⁸See, for example, G. D. Mahan, *Many-Particle Physics* (Plenum, New York, 1981), p. 397.

¹⁹S. M. Foiles and N. W. Ashcroft, J. Chem. Phys. **75**, 3594 (1981).